UNCLASSIFIED

CENTRAL RESEARCH LIBRARY
DOCUMENT COLLECTION

MARTIN MARIETTA ENERGY SYSTEMS LIBRARIES
3 4456 0349601 8

ORNL 1682
Physics Cy. 4

REACTIVITY MEASUREMENTS WITH THE BULK SHIELDING REACTOR

R. G. Cochran
J. L. Meem
T. E. Cole
E. B. Johnson

CENTRAL RESEARCH LIBRARY
DOCUMENT COLLECTION
LIBRARY LOAN COPY
DO NOT TRANSFER TO ANOTHER PERSON
If you wish someone else to see this document, send in name with document and the library will arrange a loan.

OAK RIDGE NATIONAL LABORATORY
OPERATED BY
CARBIDE AND CARBON CHEMICALS COMPANY
A DIVISION OF UNION CARBIDE AND CARBON CORPORATION
UCC
POST OFFICE BOX P
OAK RIDGE, TENNESSEE

UNCLASSIFIED

ORNL-1682

Copy No. 4

Contract No. W-7405-eng-26

REACTIVITY MEASUREMENTS WITH THE BULK SHIELDING REACTOR

R. G. Cochran

J. L. Meem

T. E. Cole

E. B. Johnson

Date Issued:

NOV 9 1954

OAK RIDGE NATIONAL LABORATORY
Operated by
CARBIDE AND CARBON CHEMICALS COMPANY
A Division of Union Carbide and Carbon Corporation
Post Office Box P
Oak Ridge, Tennessee

MARTIN MARIETTA ENERGY SYSTEMS LIBRARIES

3 4456 0349601 8

INTERNAL DISTRIBUTION

1. C. E. Center
2. Biology Library
3. Health Physics Library
4-5. Central Research Library
6. Reactor Experimental Engineering Library
7-11. Laboratory Records Department
12. Laboratory Records, ORNL R.C.
13. C. E. Larson
14. L. B. Emlet (K-25)
15. J. P. Murray (Y-12)
16. A. M. Weinberg
17. E. H. Taylor
18. E. D. Shipley
19. A. H. Snell
20. F. C. VonderLage
21. W. H. Jordan
22. J. A. Swartout
23. S. C. Lind
24. F. L. Culler
25. A. Hollaender
26. J. H. Frye, Jr.
27. W. M. Good
28. M. T. Kelley
29. G. H. Clewett
30. R. S. Livingston
31. K. Z. Morgan
32. T. A. Lincoln
33. A. S. Householder
34. C. P. Keim
35. C. S. Harrill
36. C. E. Winters
37. D. S. Billington
38. D. W. Cardwell
39. E. M. King
40. E. O. Wollan
41. A. J. Miller
42. J. A. Lane
43. R. B. Briggs
44. L. D. Roberts
45. R. N. Lyon
46. W. C. Koehler
47. E. P. Blizard
48. M. E. Rose
49. D. D. Cowen
50. W. M. Breazeale (consultant)
51. R. A. Charpie
52. M. J. Skinner
53. S. J. Cromer
54. G. E. Boyd
55. L. B. Holland
56. E. B. Johnson
57. F. C. Maienschein
58. J. L. Meem
59. H. E. Stern
60. C. L. Storrs
61. C. E. Clifford
62. H. E. Hungerford
63. K. M. Henry
64. E. P. Epler
65. S. H. Hanauer
66. T. E. Cole
67. J. D. Flynn
68. J. A. Cox
69. G. T. Chapman

EXTERNAL DISTRIBUTION

70. W. K. H. Panofsky, Stanford University
71. R. F. Bacher, California Institute of Technology
72. Division of Research and Medicine, AEC, ORO
73. R. G. Cochran, Pennsylvania State University
74. Wright Air Development Center (Attn: WCRTR, Major Sykes)
75. L. C. Widdoes, University of Michigan
76-83. W. A. Strauser, AEC, Oak Ridge
84. R. A. Anderson, AEC, Washington
85. S. W. Scott, AEC, Oak Ridge
86. Convair, Fort Worth
87. Naval Research Laboratory, Washington
88-341. Given distribution as shown in TID-4500 under Physics category

DISTRIBUTION PAGE TO BE REMOVED IF REPORT IS GIVEN PUBLIC DISTRIBUTION

Table of Contents

	ABSTRACT	1
I.	INTRODUCTION	3
II.	REACTOR	5
III.	ROD CALIBRATION VS. PERIOD	7
	BSR Regulating Rod Calibration	10
	BSR Safety Rod Calibration	15
	TSF Regulating Rod Calibration	20
	Rod Calibration by Subcritical Multiplication	23
IV.	ROD CALIBRATION VS. DISTRIBUTED POISON	28
	Gold	28
	Stainless Steel	29
V.	MEASUREMENT OF TEMPERATURE COEFFICIENT	32
VI.	MEASUREMENT OF XENON POISONING	37
VII.	TEMPERATURE STABILITY OF THE REACTOR	41
VIII.	MEGAWATT POWER LEVEL EXPERIMENTS WITH THE BSR	45
App. A.	POWER CALCULATION FOR LOADING 22	58
App. B.	ROD CALIBRATION USING STAINLESS STEEL AS A DISTRIBUTED POISON	67
	REFERENCES	79

List of Figures

Fig. No.		Page
1	Critical Loading 22A	6
2	Reactivity vs. Pile Period for a Bare Thermal Reactor as Calculated by the Inhour Equation	11
3	Differential Plot of Regulating Rod Position vs. Reactivity Change	13
4	Integral Curve of Regulating Rod Position vs. Reactivity Change; % $\Delta k/k$ from 12-in. Rod Position	14
5	Differential Plot of Safety Rod Position vs. Reactivity Change (Based on Integral Curve of Regulating Rod)	18
6	Integral Curves of Safety Rod Position vs. Reactivity Change; % $\Delta k/k$ for Inserting Rods from 22-in. Position	19
7	Integral Curve for Stainless Steel Regulating Position vs. Reactivity Change	22
8	Schematic Diagram of Thermocouple Locations for Measurement of the Temperature Coefficient of the BSR	33
9A	Temperature Coefficient of the BSR; Water Temperature vs. Regulating Rod Position	35
9B	Temperature Coefficient of the BSR; Water Temperature vs. Reactivity Change	36
10	Xenon Poisoning Experiment; Reactor Operating Time vs. Reactivity Change	40
11	Temperature Stability of the BSR; Reactor Operating Time vs. Pile Power	43
12	Stability Test of the BSR	44
13	BSR with Thermocouples and Ion Chamber in Position	47

List of Figures Cont.

Fig. No.		Page
14	Radiation Levels around Pool with BSR at 100-kw Nominal Power	48
15	Temperature Difference (ΔT) across the BSR as Measured with Thermocouples	51
16	Gamma Radiation at the Pool Surface Directly above the Reactor (16.5 ft above Core)	54
17	Bulk Shielding Reactor with Jet Diffuser in Position	55
18	Gamma Radiation from the Reactor with Jet Diffuser in Operation and Reactor at 1000 kw	57
A-1	North-South Thermal-Neutron Flux Traverses by Columns in Loading 22A-- 10-kw Nominal Power	65
A-2	Power Distribution by Rows for Loading 22A -- 10-kw Nominal Power	66

List of Tables

Table No.		Page
1	Inhour Equation Calculations for Bare Thermal Reactor	9
2	Regulating Rod Calibration by Inhour Equation	12
3	Safety Rod Calibration Data	16
4	Stainless Steel Regulating Rod Calibration Data	21
5	Data from Subcritical Multiplication Experiment	25
6	Stainless Steel--Distributed Poison Experiment	31
7	Summary of Temperature Coefficient Data	34
8	Thermocouple Data from 1-Megawatt Experiment	50
9	Gamma Radiation at the Surface of the Water Directly above the Reactor	53
10	Gamma Radiation above the Reactor--With and Without Jet Diffuser	56
A-1	Power Calculation for Loading 22A	57
A-2	Neutron Flux Traverses through the Lattice for Loading 22A	58
B-1	Calculation of Total Reactor Cross Section for Loading 22A	69

ACKNOWLEDGEMENTS

The authors gratefully acknowledge the valuable assistance given them by K. M. Henry, J. K. Leslie, J. D. Flynn and J. L. Hull in designing and installing special equipment and instrumentation and also in performing the experiments.

ABSTRACT

The Bulk Shielding Reactor has been described in detail in earlier reports. The lattice is assembled with individual fuel elements which consist of aluminum-clad plates of an aluminum-enriched uranium alloy and the necessary supporting structure. The reactor is water moderated and either water or water and beryllium oxide reflected. Recently several experiments involving reactivity changes have been performed with a water reflected lattice. The regulating rod was calibrated using both the pile period and the distributed poison methods. Excellent agreement was found between the pile period calibration using the inhour formula and the gold distributed poison, but the use of stainless steel as a distributed poison yielded results difficult to interpret. The BSR safety rods and also the control rods for the Tower Shielding Reactor were calibrated. The measurement of subcritical multiplication as a method of rod calibration was investigated qualitatively and found satisfactory at least for the comparison of different rods. The temperature coefficient of the BSR was measured between temperatures of 23 and 56°C and was found to be nonlinear, at least in this temperature range. Experiments were performed which demonstrated that the negative temperature coefficient of reactivity gives this reactor a high degree of stability at power levels greater than approximately 10 kw. The effect of xenon poisoning was investigated and found to be fairly close to that predicted by calculation. The behavior of the reactor at a power level of 1 megawatt was studied. There were no signs of boiling, even with only convection cooling. The radiation levels above the water were somewhat above Laboratory tolerance, not because of radiation from

the reactor itself, but because the water rising with a relatively high velocity from the reactor core carried the activated N^{16} and sodium in the pool water to the surface rapidly rather than allowing this activity to be dispersed throughout the pool.

I. INTRODUCTION

The Bulk Shielding Reactor has been described by Breazeale[1,2] and the reactor controls by Cole[3]. Several reports by Meem, Johnson, et al.[4,5,6] have been issued which describe the flux and power distribution in the reactor. Until the summer of 1953, the reactor was always at least partially reflected with beryllium oxide. Both prompt fission gamma rays and gamma rays from fission products produce photoneutrons from beryllium. Some of these photoneutron-producing gamma rays have half-lives comparable to the delayed neutron emitters and seriously affect the relationship between pile period and reactivity (the inhour formula). The photoneutrons produced from longer life fission products give a reactivity effect whenever there is a change in pile power, especially when the power is reduced by several orders of magnitude.

A reactor with a nearly homogeneous core immersed in an infinite medium such as water is fairly amenable to calculations. However, when the reflector is composed of several different materials (beryllium oxide and water for the BSR), reactor calculations become more complicated. No experiments involving a quantitative knowledge of reactivity changes had ever been performed with the BSR. Recently the reactor was loaded in a critical array containing no beryllium oxide and a number of experiments on reactivity changes have been performed. The regulating

rod was calibrated using both the pile period and the distributed poison method. The BSR safety rods and the control rods for the Tower Shielding Reactor were also calibrated. Measurements were made of the temperature coefficient and the xenon poisoning. Experiments were performed which demonstrated that the negative temperature coefficient of reactivity gave this reactor a high degree of stability at power levels greater than approximately 10 kw. These various experiments are described in this report.

II. REACTOR

The first 20 loadings of the BSR are listed in Appendix A of Ref. 5. Loading No. 21 was a special configuration for use with the thermal column. Loading 22 was a 5 x 6 element array with no beryllium oxide as shown in Fig. 1. The reactor contains two cadmium-lead safety rods which travel inside special elements in positions 24 and 26 and a cadmium-lead control rod located in the element in position 35. The total amount of U^{235} in the lattice was approximately 3.8 kg. The estimated critical mass for this loading was 3.5 kg. Some of the present experiments were performed with the hot set of fuel elements (previously operated at powers up to 100 kw) (loading 22A), and other experiments were performed with the cold set (never operated above 1 watt) (loading 22F). In changing from the hot set to the cold set, care was taken in loading the reactor so that the control rod positions were the same with each set of fuel elements, thus keeping the excess k in the reactor equal for either set. Hence, a given movement of the regulating rod had the same effect on the reactivity with either set of elements. The weight of fuel in each element and the flux and power distributions through the reactor are listed in Appendix A.

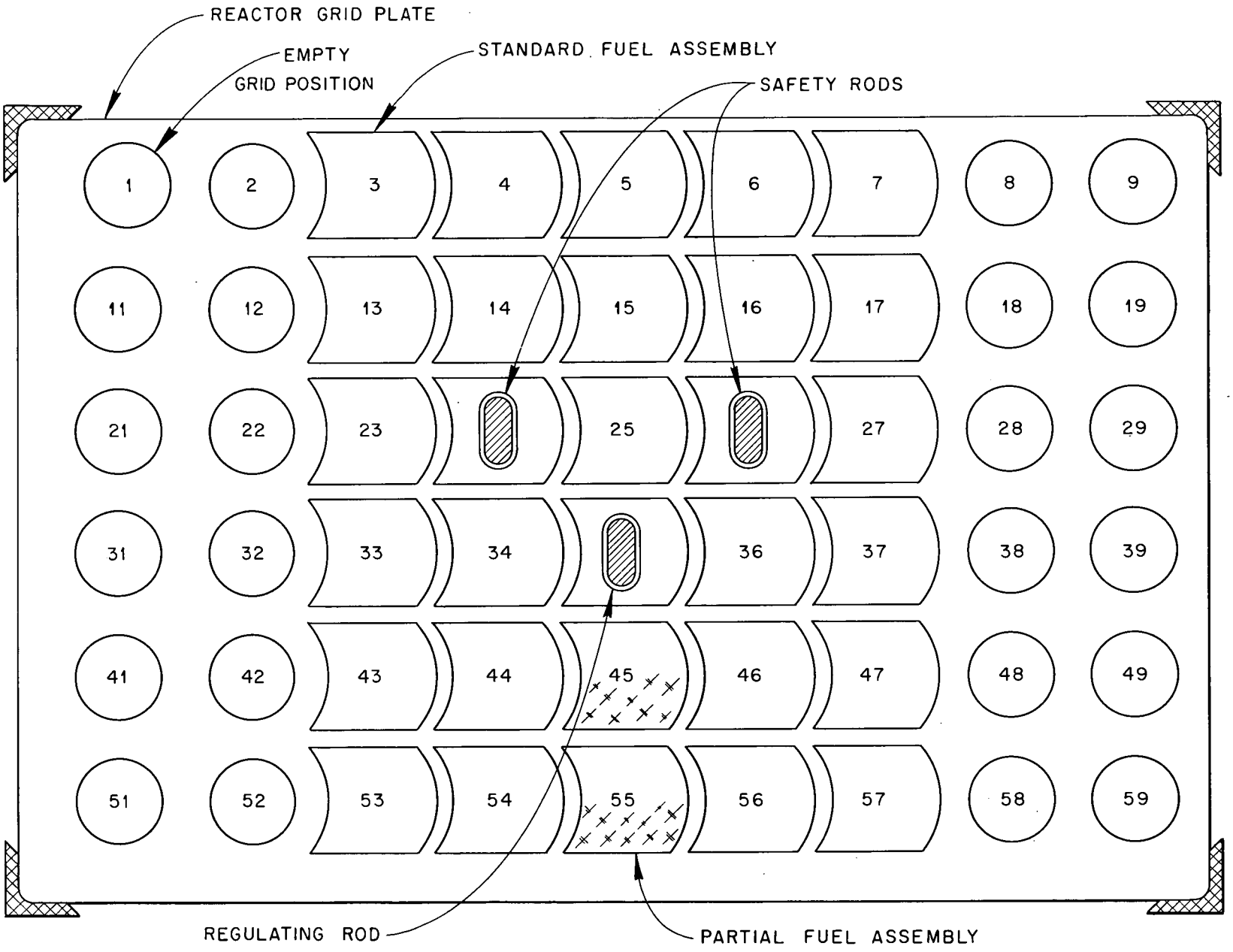

Fig. 1. Critical Loading 22A of BSR.

III. ROD CALIBRATION VS. PERIOD

The BSR normally contains two safety rods and one regulating rod, all of which are filled with a lead-cadmium mixture as the neutron-absorbing material.* The rods are approximately 26 in. long and essentially elliptical in cross section with major and minor axes of 2-1/4 and 7/8 in., respectively. The walls are made of 2S aluminum 0.065 in. thick, rolled and welded to form a waterproof shell. The safety rods are filled with a cadmium-lead mixture containing 17-1/2% cadmium. The control rod has three hollow vertical holes down the length of the rod and is filled with a mixture containing 7-1/2 g of cadmium and the remainder lead; this rod contains less absorbing material than the safety rods.

Breazeale[1] estimated that the regulating rod in the BSR would be worth 0.8% $\Delta k/k$ and that each of the two safety rods would be worth 3 to 4% for the full 24-in. travel of the rods. By means of the inhour formula, the regulating rod was calibrated against the reactor period, with the resultant curves shown in Figs. 3 and 4.

The inhour formula states the relation between reactivity and stable reactor periods as

$$\rho = \frac{\ell}{Tk_{eff}} + \sum_{i=1}^{m} \frac{\beta_i}{1 + \lambda_i T}$$

---

* ORNL Dwg. No. D-7208 shows the construction of these rods.

where

ρ = reactivity,

ℓ = average lifetime of a thermal neutron in a finite reactor,

T = stable reactor period after the transient periods have damped out,

β_i = fraction of the total fission neutrons in the ith delayed group,

λ_i = decay constant of the ith delayed neutron group.

The five definitely established delayed neutron groups were used to compute ρ for several reactor periods as shown in Table 1. Values of λ_i and β_i were taken from Table 4.8 of Glasstone and Edlund.[7] k_{eff} was taken as unity. The average lifetime ℓ of a thermal neutron in a finite reactor is the average lifetime ℓ_o in an infinite medium multiplied by the non-leakage probability of thermal neutrons, $1/(1 + L^2B^2)$. Thus

$$\ell = \frac{\ell_o}{1 + L^2B^2}$$

where

$\ell_o = 1/\Sigma_a v$,

Σ_a = macroscopic absorption cross section for thermal neutrons of velocity v,

L^2 = D/Σ_a by definition, where D is the diffusion coefficient of thermal neutrons in the medium,

B^2 = the buckling (in cm^{-1}), the lowest eigenvalue of the wave equation for the critical reactor, subject to the condition that the flux shall go to zero at the extrapolated boundary.

Table 1. Inhour Equation Calculations for Bare Thermal Reactor

$$\ell_o = \frac{1}{\Sigma_a v} = \frac{1}{2.2 \times 10^5 (0.08)} = 5.68 \times 10^{-5}$$

$$\ell = \frac{\ell_o}{1 + L^2 B^2} = \frac{5.68 \times 10^{-5}}{1.026} = 5.54 \times 10^{-5}$$

T (sec)	$\frac{\ell}{Tk_{eff}}$ x 10^4	$\sum_{i=1}^{5} \frac{\beta_i}{1 + \lambda_i T}$ x 10^4	ρ x 10^4	% $\Delta k/k$
10	0.055	28.421	28.48	0.285
15	0.037	23.564	23.60	0.236
20	0.028	20.362	20.39	0.204
30	0.0185	16.238	16.26	0.163
40	0.014	13.618	13.63	0.136
60	0.009	10.392	10.40	0.104
80	0.0069	8.445	8.45	0.0845
100	0.0055	7.128	7.13	0.071
120	0.0046	6.173	6.18	0.062
140	0.0040	5.447	5.45	0.0545
160	0.0035	4.878	4.88	0.049
200	0.0028	4.035	4.038	0.040
250	0.0022	3.321	3.32	0.033
300	0.0018	2.823	2.825	0.028

Figure 2 is the plot of reactivity versus reactor period as given in the inhour formula for a bare thermal reactor.

BSR Regulating Rod Calibration

The regulating rod calibration was carried out in the following way. The reactor was brought up to 10 watts power level and allowed to stabilize for at least 5 min. The reactor was put on manual control and the regulating rod was withdrawn as quickly as possible to a predetermined position with, of course, no movement of the safety rods. The reactor period was observed between power levels of 100 watts and 1 kw. It was assumed that the effect of the transient terms on the reactor period would damp out in the interval between 10 and 100 watts and that there would be no temperature effect on the period at 1 kw. The reactor was scrammed at 10 kw and the procedure repeated for several settings of the regulating rod. It was necessary, of course, to adjust the positions of the safety rods between the different runs in order to obtain the calibration of the regulating rod over 12 in. of its travel. The change in reactivity corresponding to the observed reactor period was obtained from Fig. 2. Table 2 is a summary of the regulating rod calibration data. R_1 and R_2 are the initial and final positions of the regulating rod, ΔR is the change in rod position, T_R is the observed reactor period corresponding to this change, and % $\Delta k/k$ per inch is the change in reactivity for each inch of rod movement. As can be seen from Figs. 3 and 4, the rod is worth 0.6% $\Delta k/k$ for a travel of 12 in. The regulating rod gives anomalous results when inserted further than 12 in. and actually gives a reversal in reactivity. This anomaly has not been completely investigated at

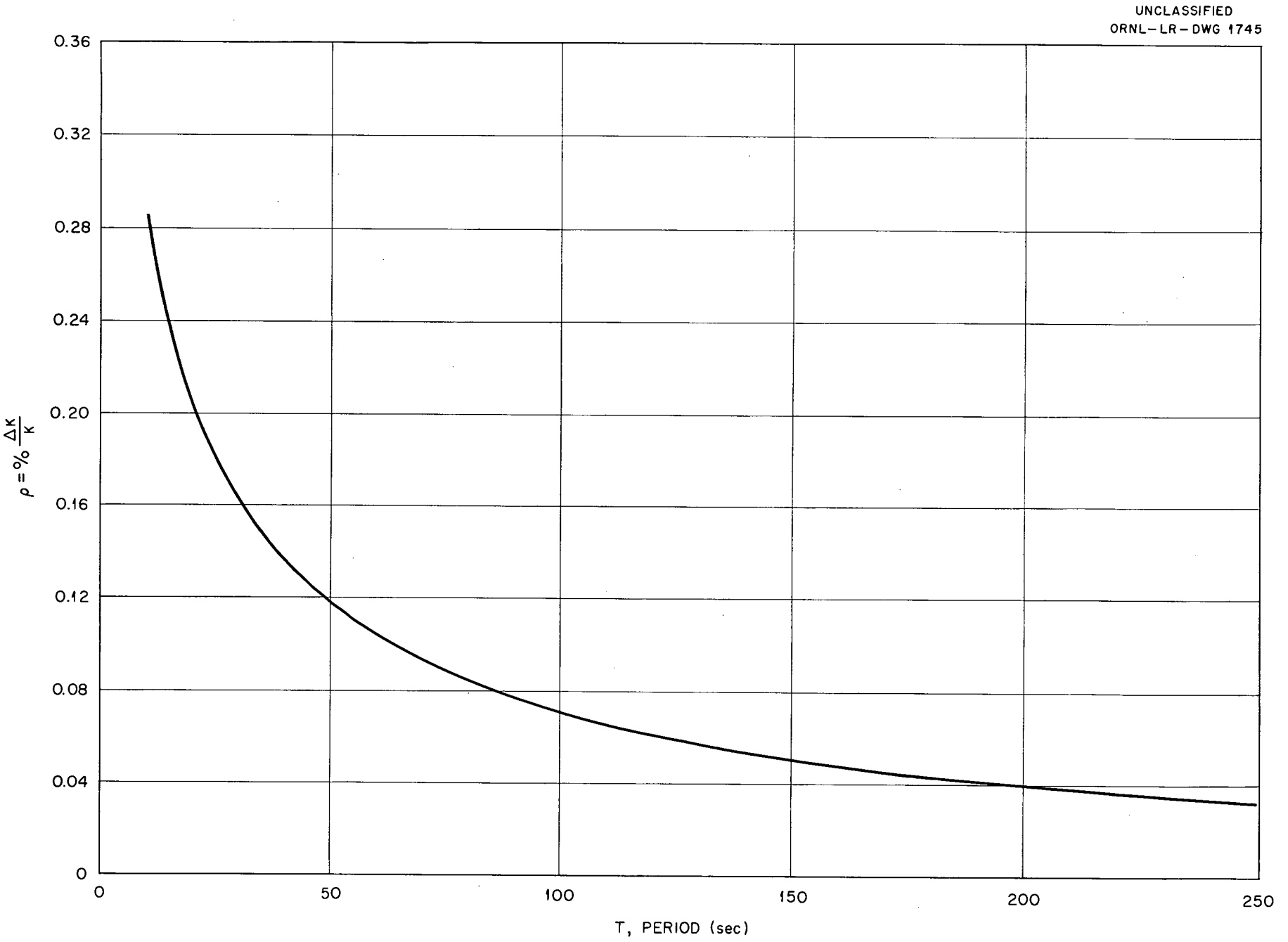

Fig. 2. Reactivity vs. Pile Period for a Bare Thermal Reactor as Calculated by the Inhour Equation $\rho = \frac{\ell}{TK_{EFF}} + \sum_{i=1}^{5} \frac{\beta_i}{1+\lambda_i T}$

Table 2. Regulating Rod Calibration by Inhour Equation

Run Number	Reading	R_1 (in.)	R_2 (in.)	ΔR (in.)	T_R (sec)	$\frac{\% \Delta k/k}{in.}$
3	1	12	13	1	95.8	0.0735
	2	12	15	3	16.1	0.076
	3	12	14	2	36.55	0.072
	4	13	14	1	92.9	0.0755
	5	13	15	2	33.5	0.076
	6	13	16	3	16.36	0.075
	7	14	15	1	88.0	0.078
	8	14	16	2	32.75	0.077
	9	15	17	2	33.28	0.076
	10	16	18	2	37.5	0.071
	11	11	13	2	44.25	0.064
28	1	18	20	2	61	0.0515
	2	18	19	1	146	0.052
	3	18	21	3	36	0.048
	4	19	20	1	180	0.044
	5	19	21	2	79	0.0425
	6	20	22	2	125	0.030
	7	21	23	2	174	0.0225
	8	22	24	2	270	0.015

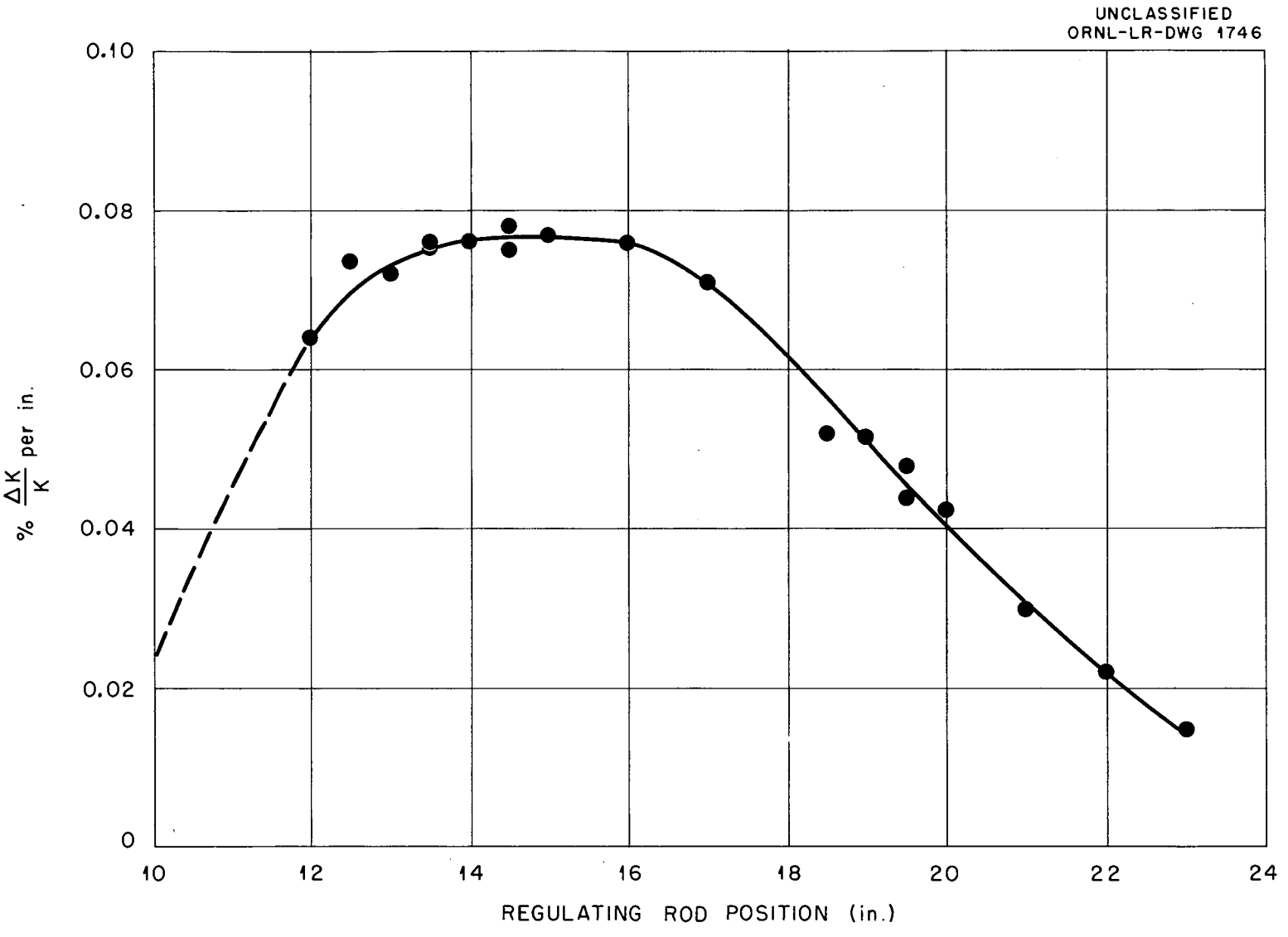

Fig. 3. Differential Plot of Regulating Rod Position vs. Reactivity Change.

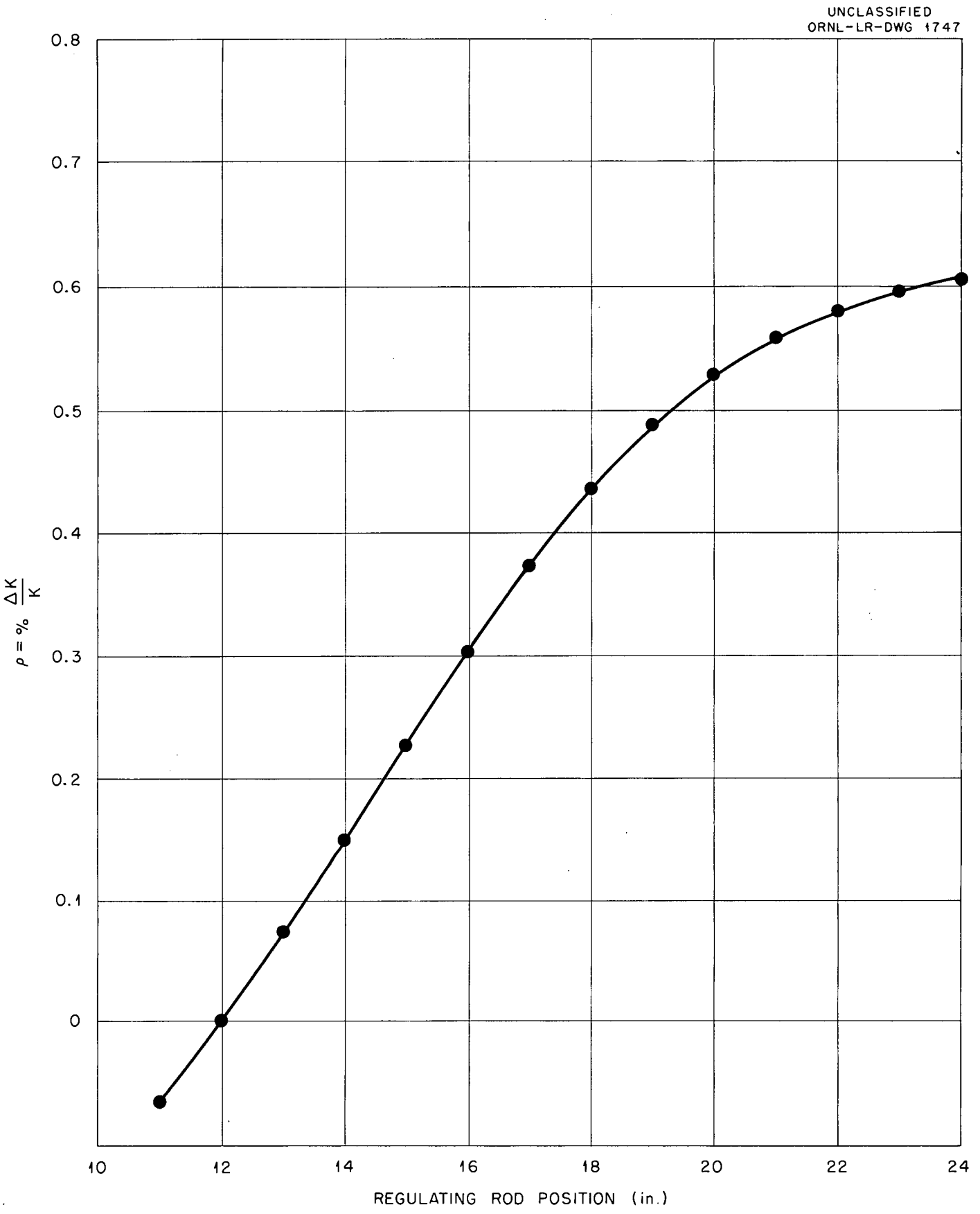

Fig. 4. Integral Curve of Regulating Rod Position vs. Reactivity Change; % $\frac{\Delta K}{K}$ from 12-in. Rod Position.

this time.

It should be pointed out that, since the relative positions of the safety rods and the regulating rod were of necessity changed in the process of obtaining the control rod data, the resulting calibration reflects the effect of these changes and is not a true measure of the worth of the regulating rod. No attempt has been made to evaluate the effect of the "shading" of one rod by another in this lattice or to correct for this effect, but it is believed that this effect is relatively small.

BSR Safety Rod Calibration

The safety rods were calibrated against the regulating rod. For this experiment the reactor was brought to a power of 100 watts, put on servo, and allowed to stabilize. The positions of the two safety rods and the regulating rod were noted. Then one of the safety rods was moved, causing the servo to move the regulating rod to a new position in order to maintain constant power. The new rod positions were noted. This procedure was repeated with each safety rod until sufficient data was obtained. The change in reactivity corresponding to a given movement of a safety rod was obtained from the integral curve for the regulating rod (Fig. 4). Table 3 is a summary of the calibration data for the safety rods and Fig. 5 is a plot of this data. Figure 6 shows the integral curve for each safety rod. According to this calibration, each safety rod is worth approximately 1.3% $\Delta k/k$ for 20 in. of travel.

Table 3. Safety Rod Calibration Data

Regulating Rod Position (in.)	Δ RR (in.)	Safety Rod No. 1		Safety Rod No. 2		Plotting Point
		Position (in.)	% Δk/k / in.	Position (in.)	% Δk/k / in.	
			Safety Rod No. 1			
17.7 18.7	1.6	16 15	0.092	16 16		15.5
16.3 18.7	2.4	17 15	0.074	16 16		16.0
20.8 17.3	3.5	15 17	0.079	15 15		16.0
16.8 20.8	4.0	18 15	0.064	15 15		16.5
20.8 16.2	4.6	15 19	0.0585	15 15		17.0
17.3 16.2	1.1	17 19	0.039	15 15		18.0
13.3 14.7	1.4	19 17	0.054	18 18		18.0
20.8 15.4	5.4	15 22	0.042	15 15		18.5
17.3 15.4	1.9	17 22	0.027	15 15		19.5
16.2 15.4	0.8	19 22	0.020	15 15		20.5
15.9 15.4	0.5	20 22	0.0185	15 15		21.0

Table 3 Con't.

Regulating Rod Position (in.)	Δ RR (in.)	Safety Rod No. 1		Safety Rod No. 2		Plotting Point
		Position (in.)	% Δk/k / in.	Position (in.)	% Δk/k / in.	
Safety Rod No. 2						
18.7 21.0	2.3	15 15		16 15	0.085	15.5
21.0 17.3	3.7	15 15		15 17	0.082	16.0
14.7 16.3	1.6	17 17		18 16	0.061	17.0
17.3 15.9	1.4	15 15		17 19	0.049	18.0
21.0 15.0	6.0	15 15		15 22	0.047	18.5
12.1 13.3	1.2	19 19		20 18	0.044	19.0
15.9 15.1	0.8	15 15		19 21	0.0305	20.0
15.4 15.0	0.4	15 15		20 22	0.0155	21.0

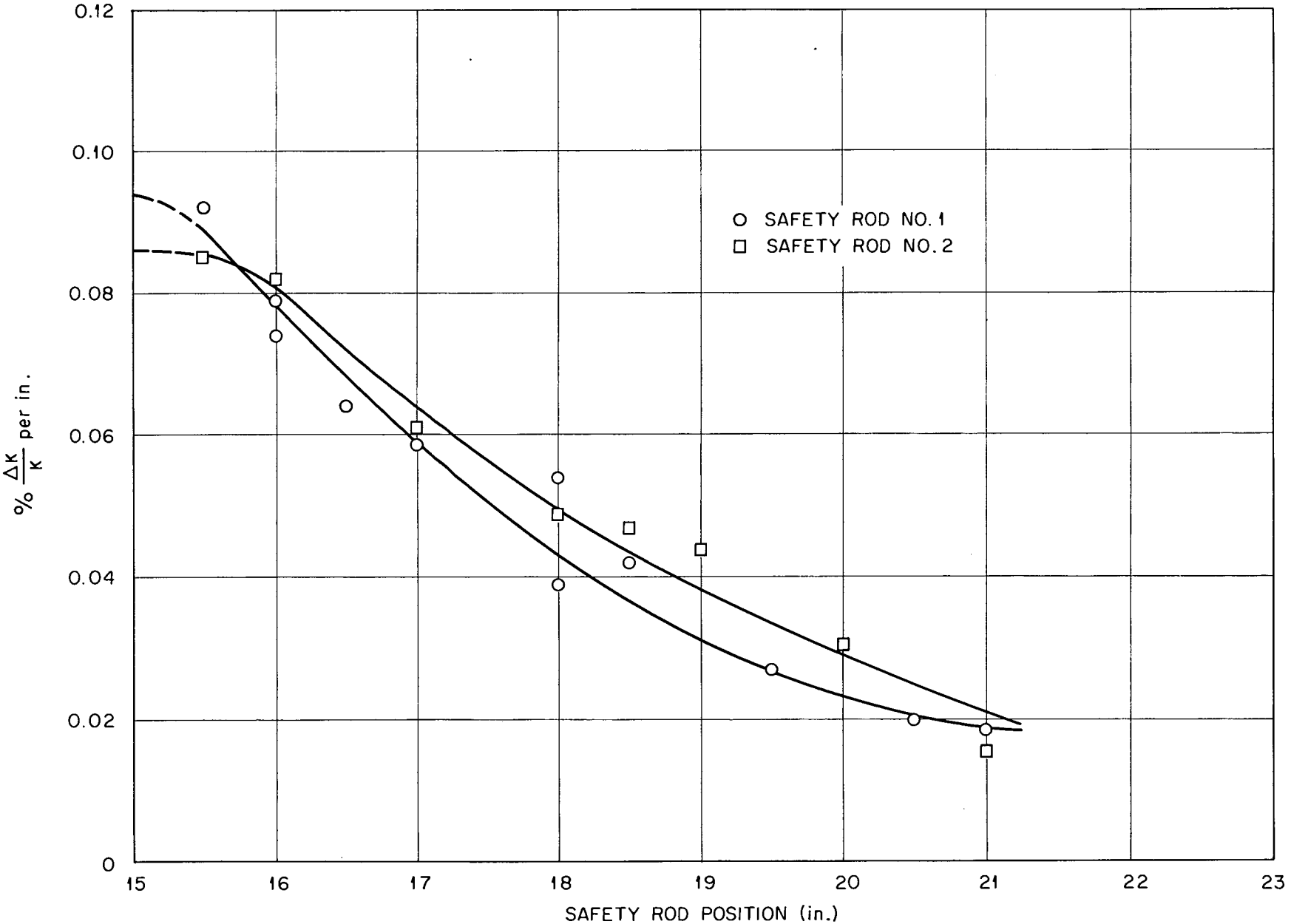

Fig. 5. Differential Plot of Safety Rod Position vs. Reactivity Change. (Based on Integral Curve of Regulating Rod)

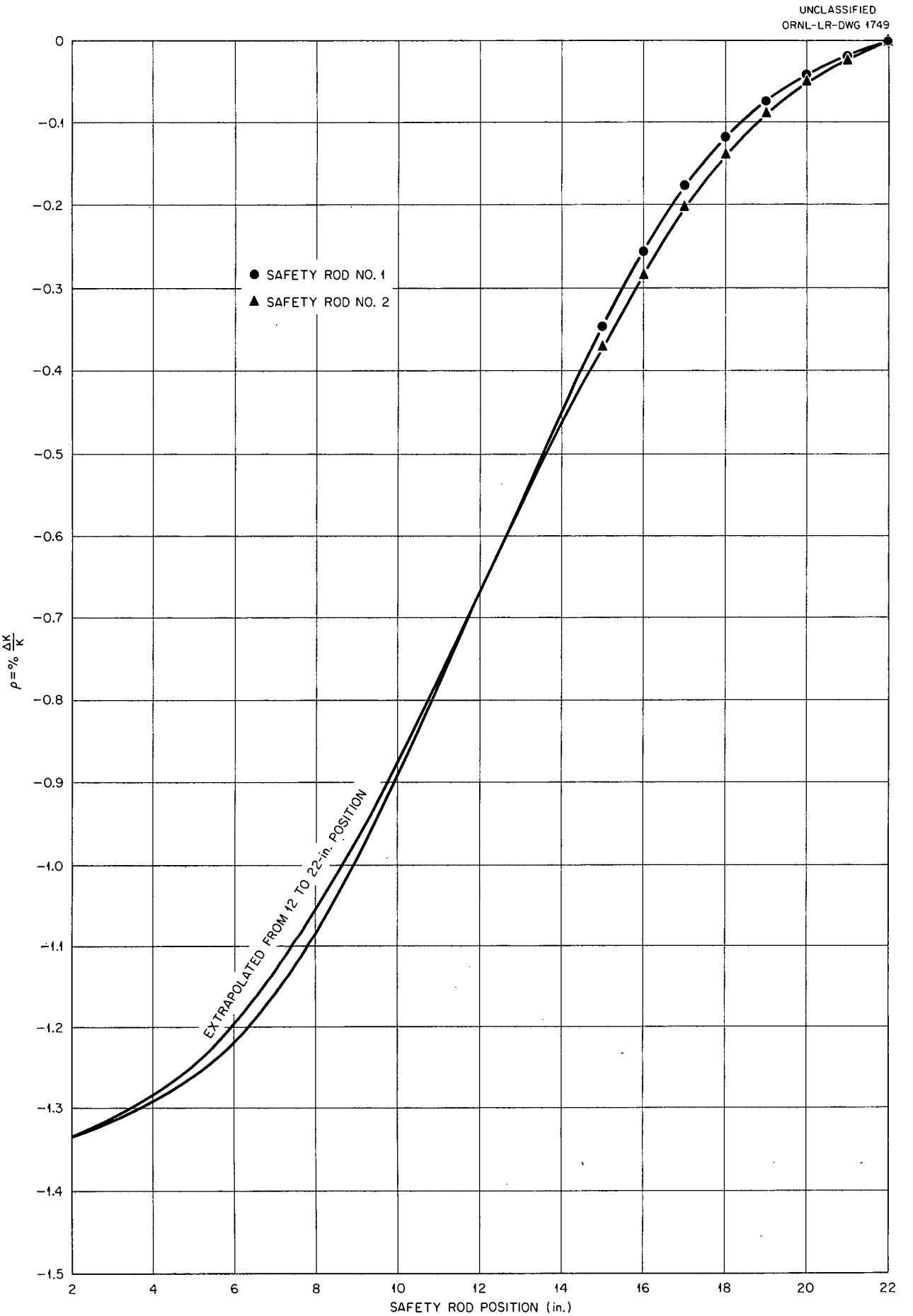

Fig. 6. Integral Curves of Safety Rod Position vs. Reactivity Change; % $\frac{\Delta K}{K}$ for Inserting Rods from 22-in. Position.

TSF Regulating Rod Calibration

In addition to the calibration of the standard BSR regulating rod, a rough check was made on a regulating rod which contained type 347 stainless steel as the absorbing material.* The stainless steel was in the form of a cylinder 1.5 in. ID and 24.875 in. long with a wall thickness of 0.065 in. This cylinder was sandwiched between two cylinders of aluminum and rolled to approximately the same outside dimensions as the standard BSR regulating rod. The inner aluminum cylinder had a wall thickness of 0.065 in. and the outer cylinder 0.049 in. The weight of stainless steel was approximately 1 kg. The reactor was loaded with the hot elements (loading 22A) and, in addition to the stainless steel regulating rod, contained a B_4C-loaded rod which had been substituted for the No. 2 BSR safety rod.

The calibration was carried out as described above for the BSR control rod. The reactor was brought to a power level of 10 watts with the regulating rod at the desired initial position. After making certain that steady-state operation had been attained, the regulating rod was withdrawn the desired amount and the reactor period measured between 100 watts and 1 kw. The data is presented in Table 4 and a curve plotted from the data is shown as Fig. 7. The conversion from period to $\Delta k/k$ was taken from Fig. 2. It should be noted that this rod does not exhibit the anomaly noted for the standard BSR rod.

---

* ORNL Dwg. No. D-14468 Rev. A shows the construction of the rod.

Table 4. Stainless Steel Regulating Rod Calibration Data

RR Displacement (in.)	Initial Safety Rod Positions (in.)		Period (sec)	% Δk/k
	No. 1	No. 2		
0 to 9	17	17.6	31.3	0.158
9 to 13	14.9	16.8	56.9	0.108
13 to 17	15.3	16.1	78.2	0.086
17 to 23.5	15^{+}	15.9	145.9	0.052
			Total	0.404% Δk/k

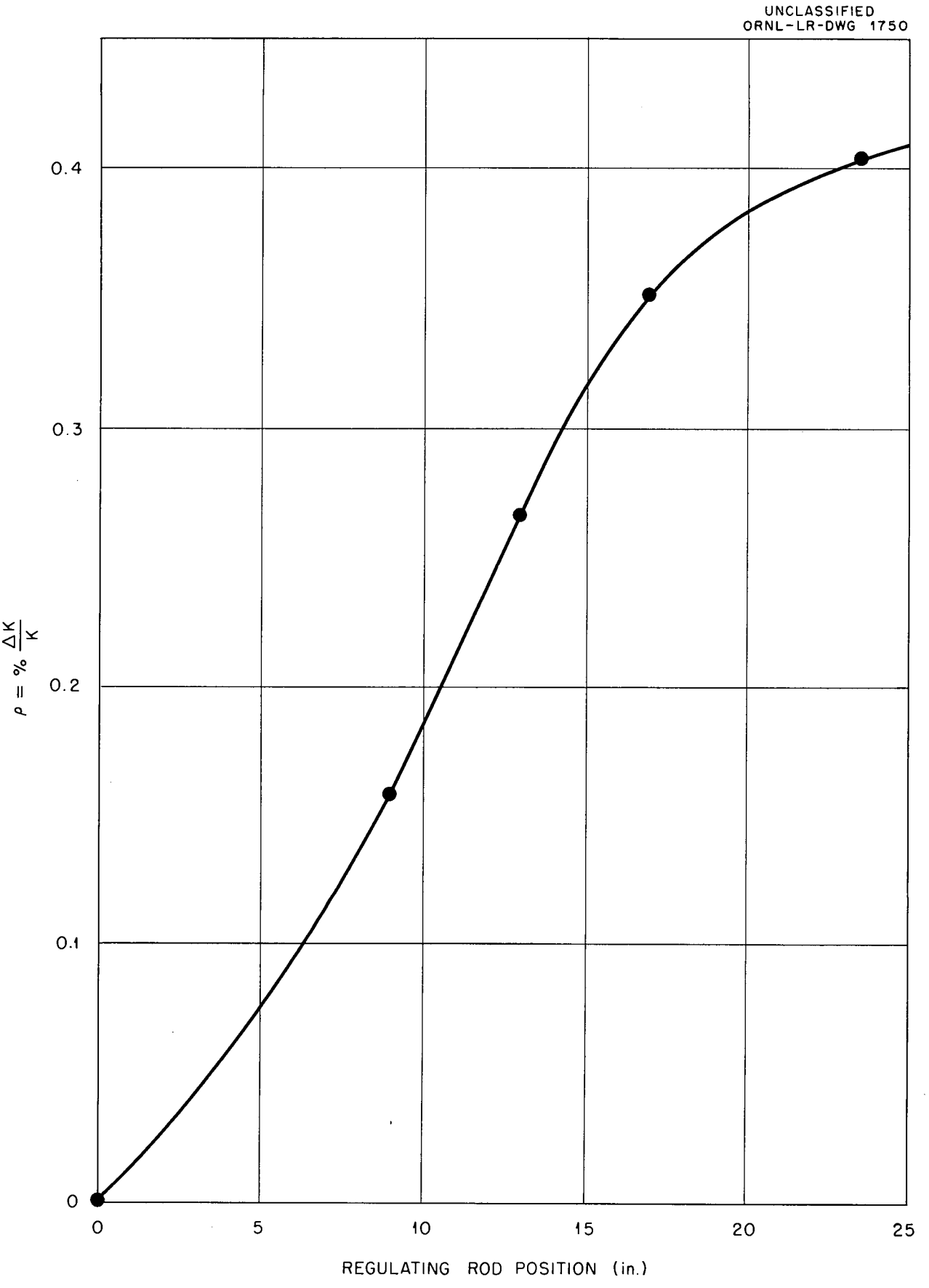

Fig. 7. Integral Curve for Stainless Steel Regulating Rod Position vs. Reactivity Change.

The results are to be taken as semiquantitative and as representing an average operating condition. No corrections have been made for the fact that it was necessary to move the safety rods each time the initial position of the regulating rod was changed. The positions of the shims are given in Table 4 for each initial regulating rod position.

Rod Calibration by Subcritical Multiplication

There were two reasons for performing this experiment: (1) to gain information as to the feasibility of rod calibration by the measurement of subcritical multiplication, and (2) to obtain a rough check on the relative effectiveness of the standard BSR lead-cadmium safety rod* and a rod of similar dimensions but loaded with B_4C.**

The reactor was loaded as described above and shown in Fig. 1 with two exceptions. The stainless steel regulating rod discussed in the previous section was substituted for the BSR regulating rod and the No. 2 safety rod contained B_4C as the absorbing material; the No. 1 safety rod was the standard lead-cadmium BSR rod.

Since it was necessary to know the effectiveness of the stainless steel regulating rod, a calibration of this rod was made using the inhour relationship as described above. Thus it was known that the amount of $\Delta k_{eff}/k_{eff}$ introduced when the rod was moved from fully withdrawn to fully inserted was -0.00404 (see Table 4 and Fig. 7).

A polonium-beryllium source was located on the opposite side of the reactor from the fission chamber so that a large portion of the

---

* Refer to ORNL Dwg. No. D-7208.

** Refer to ORNL Dwg. No. D-14468, Rev. A.

multiplying medium was between the source and the counter. The counting rate of the fission chamber due to the source was observed with all rods fully inserted. The safety rods were then withdrawn various distances and the counting rate was observed as a function of safety rod position (see Table 5). The reactor was then brought to criticality with the regulating rod fully withdrawn. When steady-state conditions were obtained the regulating rod was fully inserted and counts were taken when the reactor again attained a steady power level (subcritical).

The subcritical multiplication $M = 1/(1-k_{eff})$ and the observed counting rate of the fission chamber (Run 15 in Table 5) were used to calculate an effective source strength:

$$\left(\frac{\Delta k_{eff}}{k_{eff}}\right)_{RR} = -0.00404$$

$$k_{eff} = \frac{1}{1.00404} = 0.99598$$

$$M = \frac{1}{1 - k_{eff}} = \frac{1}{1 - 0.99598} = 248.8$$

$$S_{eff} = \frac{\text{Counting rate}}{\text{Multiplication}} = \frac{551.5}{248.8} = 2.217$$

The effective source strength S_{eff} and the observed counting rate for various positions of the rods (subcritical) were used to determine the k_{eff} for each of the positions. Table 5 lists these values.

This data should be regarded as presenting a rough survey and no evaluation has been made of the errors which may enter through such

Table 5. Data from Subcritical Multiplication Experiment

Run No.	Regulating Rod Position (in.)	Safety Rod Positions (in.)		CPM	M	k_{eff}
		No. 1	No. 2			
1	0.0	0.0	0.0	45.33	20.447	0.9511
2	0.0	6.0	6.0	59.61	26.888	0.9628
3	0.0	8.0	8.0	67.68	30.528	0.9672
4	0.0	10.0	10.0	81.69	36.847	0.9729
5	0.0	12.0	12.0	104.9	47.316	0.9789
6	0.0	14.0	14.0	179.3	80.875	0.9876
7	0.0	16.0	16.0	320.5	144.565	0.9930
8	0.0	18.0	16.0	427.3	192.74	0.9948
9	0.0	18.0	18.0	960.0	433.02	0.9977
10	0.0	19.0	18.0	1309.5	590.7	0.9983
11	0.0	19.0	19.0	3720	1678	0.9994
12	0.0	19.5	19.0	7039	3175	0.99968
13	0.0	19.5	19.23	Probably just critical		
14	23.5	17^+	17.2	55050	(1 watt)	
15	0	17^+	17.2	551.5	248.76	0.99598
16	0	12.0	12.0	114.2	51.511	0.9806
17	0	≈25.2	0	90.2	40.686	0.9754
18	0	0	≈24.5	159.4	71.899	0.9861

factors as the relative positions of source, fission chamber, and rods.

Runs 5 and 16 should be a check on the reproducibility of the method as applied to this experiment as they were made several hours apart. Let k_i be the k_{eff} obtained under conditions of the ith run (see Table 5).

$$k_5 = 0.9789$$

$$k_{16} = 0.9806$$

$$k_{16} - k_5 = 0.0017$$

The difference indicates that the measurement of k_{eff} was reproducible in this case to about 17 parts in 10^4.

It will be recalled that the inhour calibration of the BSR safety rods indicated that the two rods were quite similar. Therefore, a comparison of the effectiveness of the No. 1 rod (the standard BSR rod) and the No. 2 rod (the B_4C-loaded rod), as indicated by subcritical multiplication, should be valid.

$k_8 - k_7 =$ 0.0018; Rod No. 1 from 16 to 18 in.; 0.0009 $(\Delta k/k)$/in.

$k_9 - k_8 =$ 0.0029; Rod No. 2 from 16 to 18 in.; 0.00145 $(\Delta k/k)$/in.

$k_{10} - k_9 =$ 0.00061; Rod No. 1 from 18 to 19 in.; 0.00061 $(\Delta k/k)$/in.

$k_{11} - k_{10} =$ 0.00109; Rod No. 2 from 18 to 19 in.; 0.00109 $(\Delta k/k)$/in.

$k_{12} - k_{11} =$ 0.00028; Rod No. 1 from 19 to 19.5 in.; 0.00056 $(\Delta k/k)$/in.

The inhour calibration of the No. 1 safety rod described previously indicated the following values for the same increments:

From 16 to 18 in., $(\Delta k/k)/\text{in.} = 0.00069$; cf. $k_8 - k_7$

From 18 to 19 in., $(\Delta k/k)/\text{in.} = 0.00052$; cf. $k_{10} - k_9$

From 19 to 19.5 in., $(\Delta k/k)/\text{in.} = 0.00038$; cf. $k_{12} - k_{11}$

A comparison between Rod No. 1 and Rod No. 2 in terms of $\Delta k/k$ per inch shows that Rod No. 2 is more effective by a factor of at least 1.5.

At this point emphasis must be given to the fact that this experiment was done in a qualitative manner and the data and results should be treated as such.

While the accuracy of the method of subcritical multiplication for absolute calibration of rods has not been established by this exploratory experiment, the method is of definite value for the comparison of the relative effectiveness of different rods.

IV. ROD CALIBRATION VS. DISTRIBUTED POISON

Gold

One check on the rod calibration previously mentioned, using the inhour formula, was obtained by using gold as a distributed poison in the reactor. The poisoning was accomplished by taping 0.25-g. gold foils on each side of the cold fuel elements in loading 22F (Fig. 1). With the reactor critical, the position of the regulating rod was noted before adding the gold foils and again after the poison was put into the reactor. If the addition of poison has negligible effect on the Fermi age and the thermal diffusion length of the neutrons, the change in reactivity is caused only by the change in thermal utilization. Therefore

$$\frac{\Delta k}{k} = \frac{\Delta f}{f} = \frac{\Delta \Sigma_R}{\Sigma_R}$$

where Σ_R is the total absorption cross section for the reactor. As calculated in Appendix B, the total reactor cross section was

$$\Sigma_R = 8775 \text{ cm}^2$$

A total of 71.55 g of gold distributed uniformly throughout the reactor core resulted in a regulating rod position of 14.85 in.; with no gold in the lattice the regulating rod position was 11.7 in.

$$\sigma_{Au} = 98 \times 10^{-24}\ cm^2 \text{ for 2200-m/sec neutrons}^{(8)}$$

$$\Sigma_{Au} = \frac{(98 \times 10^{-24}\ cm^2/atom)\ (6.02 \times 10^{23}\ atoms/mol)}{197\ g/mol} = 0.299\ cm^2/g$$

$$\Delta\Sigma = (0.299\ cm^2/g)\ (71.55\ g) = 21.39\ cm^2$$

$$\frac{\Delta k}{k} = \frac{\Delta\Sigma}{\Sigma} = \frac{21.39}{8775} = 0.002437$$

According to the inhour calibration of the control rod (Fig. 4), a movement of the rod from 11.7 to 14.85 in. corresponds to a change in reactivity of 0.235%, in good agreement with that indicated by the gold poison.

Stainless Steel

With the cold reactor loading, poison in the form of stainless steel strips was distributed throughout the reactor. The strips were inserted between the fuel plates in 27 of the 30 fuel elements; it was impractical to insert strips in the three rod elements. The strips were 25 in. long and 1/32 in. thick, with a 1-3/8 in. long aluminum cylinder 3/8 in. in diameter attached to each strip 3/8 in. below the top with an aluminum pin. Three sets of strips were used and the strips within each set were extremely uniform. The total weights of stainless steel adjacent to the uranium-containing portion of the fuel plates were 1390.35, 858.9 and 406.7 g, respectively, for the three sets.

In order to measure the effect of this distributed poison in

terms of movement of the regulating rod, the reactor was made just critical with no poison (at a power level of 1 watt), and allowed to stabilize, and the rod positions were noted. The reactor was shut down and the 27 strips of one set were inserted into the elements. The reactor was then brought back to criticality with the safety rods at their previous positions, allowed to stabilize, and the new regulating rod position noted. This procedure was repeated for each of the three sets of stainless steel strips. The calculations are shown in detail in Appendix B. Table 6 is a summary of the results.

In each of the three cases the value for reactivity taken from the inhour calibration of the regulating rod falls between the values obtained by calculating $\Delta k_\infty/k_\infty$ and $\Delta k_{eff}/k_{eff}$ due to putting stainless steel in the core.

It should be noted that the assumption was made that the scattering cross sections for stainless steel were the same as those for aluminum and therefore that the change in η would be the same as if an equal volume of aluminum were put in the reactor. This is probably not a good assumption and should be investigated in greater detail when time permits. This is probably a major source of error in calculating the $\Delta k_{eff}/k_{eff}$ due to insertion of the stainless steel.

Table 6. Stainless Steel--Distributed Poison Experiment

Case No.	Amount of 347SS (g)	Change in Reactivity		
		From Inhour Calibration of Regulating Rod, $\frac{\Delta k_{eff}}{k_{eff}}$	From Change in Thermal Utilization, $\frac{\Delta k_{\infty}}{k_{\infty}}$	From Change in η, $\frac{\Delta k_{eff}}{k_{eff}}$
1	1390.35	0.00483	0.00456	0.00593
2	858.9	0.00309	0.00281	0.00366
3	406.7	0.00143	0.00133	0.00173

V. MEASUREMENT OF TEMPERATURE COEFFICIENT

For this experiment, the reactor was placed behind the aluminum gate in the small pool (see Ref. 1) and the large section of the pool was drained. The water in the small pool was heated by passing steam in at the bottom of the pool at the rate of 10,000 lb/hr. Thermocouples were installed at a number of positions around the reactor as shown in Fig. 8. The reactor was held at a constant power of 100 watts by the servo and the withdrawal of the regulating rod noted as the water temperature increased because of the introduction of the steam. At this power, no appreciable heat was generated by the reactor itself, and the reactor was considered to be at essentially uniform temperature throughout. The average of all thermocouple readings was considered the reactor temperature. Table 7 is a summary of the data. During the experiment, the water temperature was increased from 17.7 to 56°C. The resultant change in reactivity as determined from withdrawal of the calibrated rod is shown in Figs. 9A and 9B. The temperature coefficient as indicated by the curve in Fig. 9B is not a constant, even over the temperature range investigated; at 26°C the temperature coefficient is -6×10^{-5}, while at 55°C it is at least -10×10^{-5}. If only the end points of the curve are used, the average temperature coefficient is -8×10^{-5} per degree centigrade.

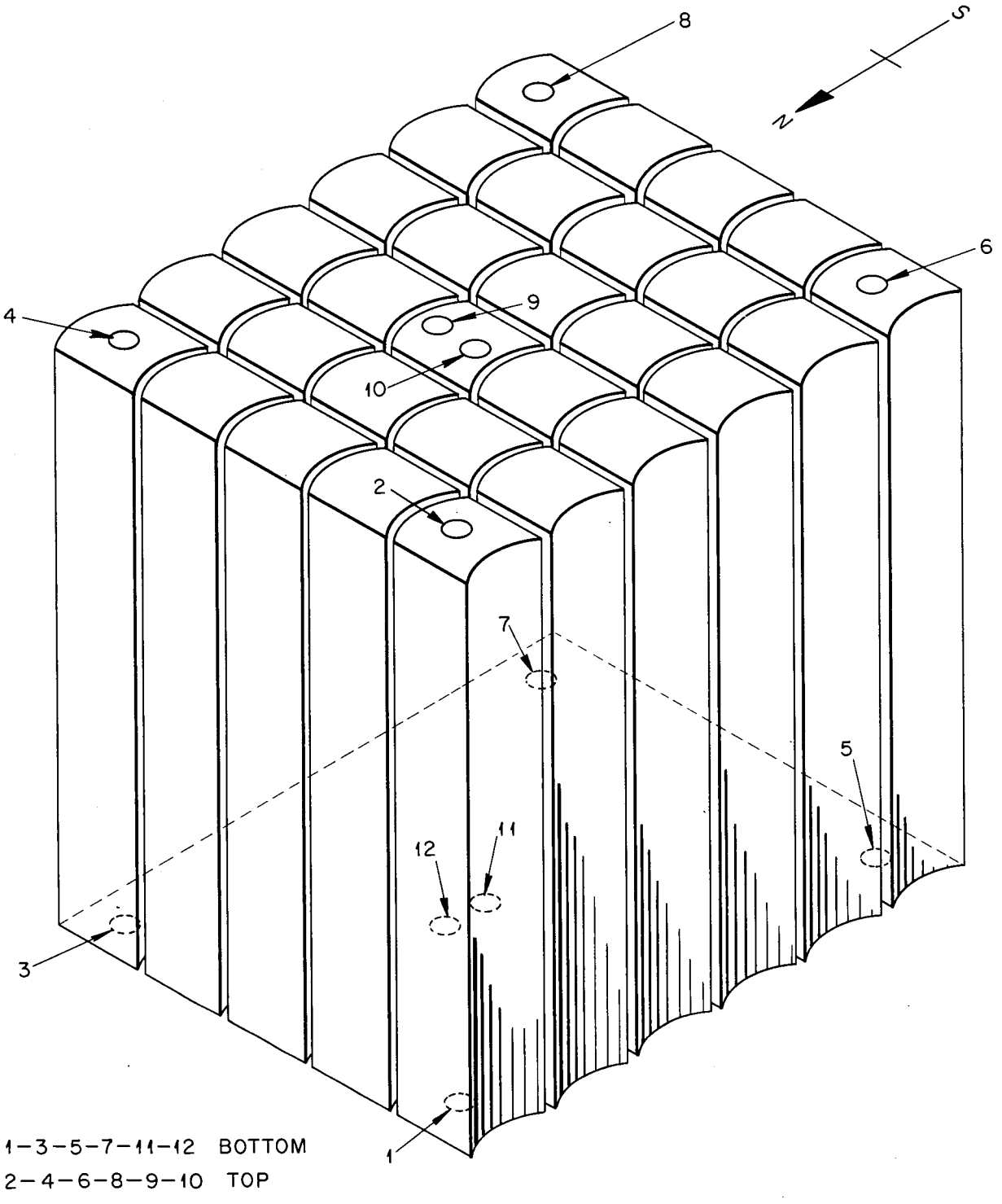

Fig. 8. Schematic Diagram of Thermocouple Locations for Measurement of the Temperature Coefficient of the BSR.

Table 7. Summary of Temperature Coefficient Data

10,000 lb steam/hr

Time	Regulating Rod Position (in.)	Average Temperature (°C)
0931-0937[a]	0	17.4
1000[a]	12	17.7
1010[a]	12	17.65
1020[b]	12	17.7
1030	11.9	19.1
1040	11.8 - 11.9	21.2
1050	12.0	23.0
1100	12.1 - 12.2	24.85
1110	12.2 - 12.3	26.6
1120	12.3 - 12.5	28.2
1130	12.5 - 12.7	30.1
1140	12.7 - 12.8	31.9
1150	12.8 - 13.0	33.63
1200	13.0 - 13.2	35.17
1210	13.2 - 13.3	36.87
1220	13.3 - 13.5	38.36
1230	13.6	40.07
1240	13.8	41.65
1250	13.9	43.26
1300	14.05	44.5
1310	14.25	46.07
1321		47.13
1330	14.6	47.93
1340	14.5 - 14.7	48.90
1350	14.7 - 14.8	49.91
1400	14.7 - 14.9	51.05
1410	14.9 - 15.1	52.17
1420	15.0 - 15.2	53.43
1430	15.4	54.84
1440[c]	15.6	56.00

(a) No steam.
(b) Steam started at 1020.
(c) Steam off at 1448.

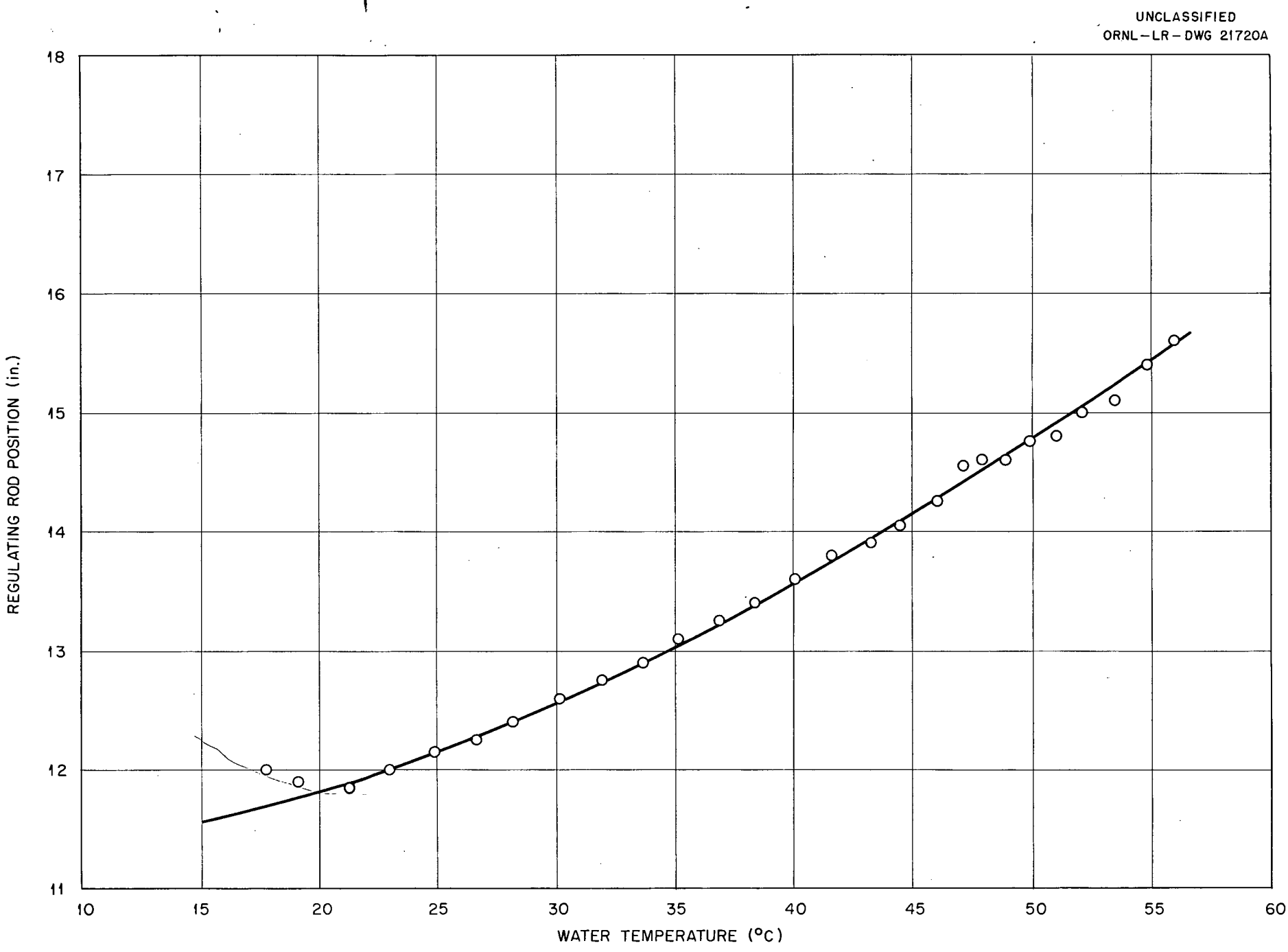

Fig. 9A. Temperature Coefficient of the BSR; Water Temperature vs. Regulating Rod Position.

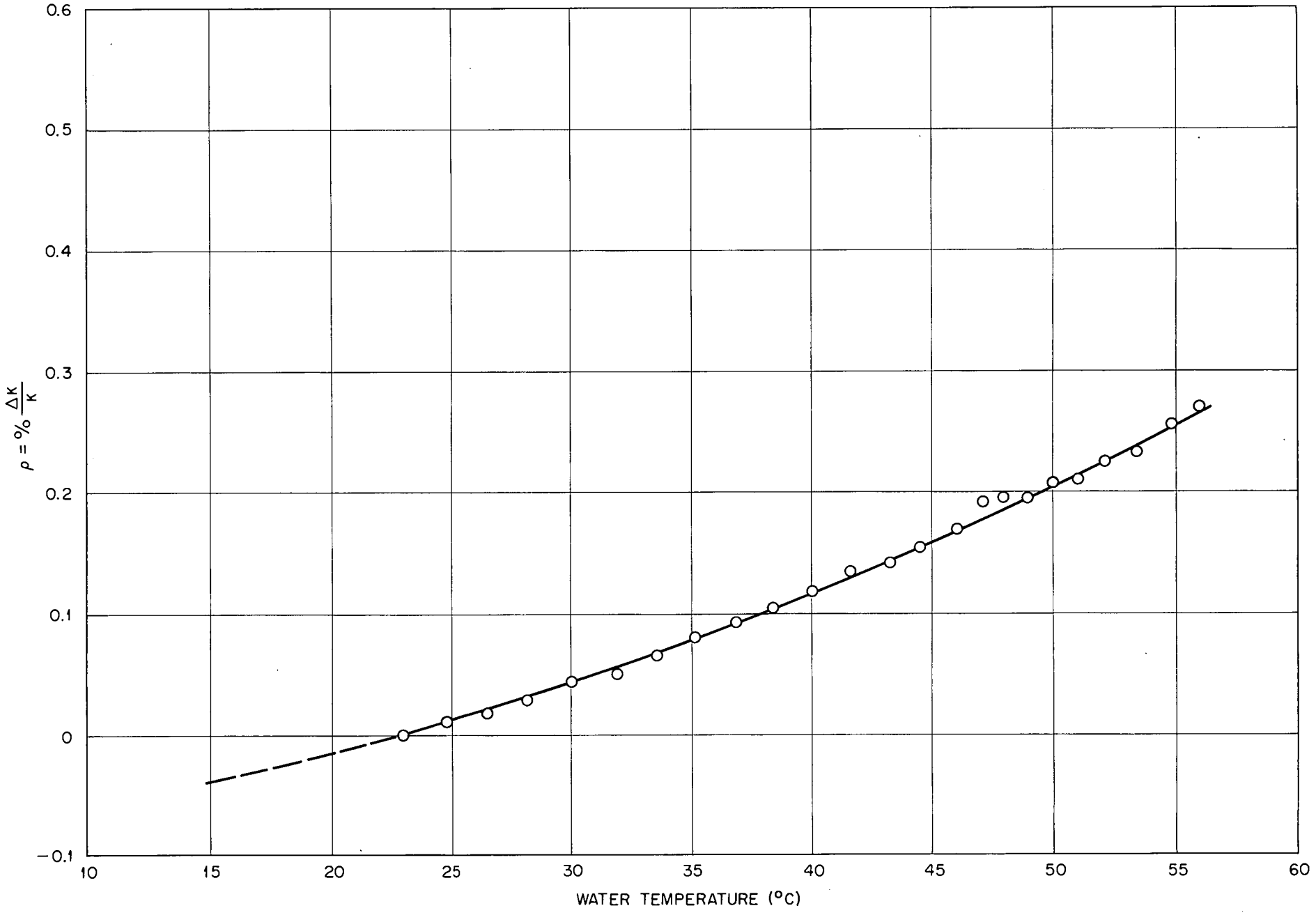

Fig. 9B. Temperature Coefficient of the BSR; Water Temperature vs. Reactivity Change.

VI. MEASUREMENT OF XENON POISONING

The poisoning P of a reactor is defined by Glasstone and Edlund[7] as the ratio of the number of thermal neutrons absorbed by the poison to those absorbed in the fuel. Hence, the poisoning P_o due to Xe^{135}, when the latter has reached equilibrium, is:

$$P_o = \frac{X_o \sigma_2}{\Sigma_U} = \frac{\sigma_2(\gamma_1 + \gamma_2)\Sigma_f \phi_o}{(\lambda_2 + \sigma_2 \phi_o)\Sigma_U}$$

where

$$X_o = \frac{(\gamma_1 + \gamma_2)\Sigma_f \phi_o}{\lambda_2 + \sigma_2 \phi_o}$$

γ_1 = fractional yield of I^{135} as a direct fission product

= 5.6%,

γ_2 = fractional yield of Xe^{135} as a direct fission product

= 0.3%,

Σ_f = macroscopic fission cross section,

Σ_U = mascroscopic thermal absorption cross section in fuel,

ϕ_o = average thermal-neutron flux

= 7.36×10^{11} neutrons/cm^2/sec at 118 kw,

σ_2 = Xe^{135} microscopic thermal absorption cross section

= 3.5×10^{-18} cm^2,

λ_2 = decay constant for Xe^{135}

= 2.1×10^{-5} sec^{-1}.

The change in reactivity ρ is the product of the poisoning P_o and the thermal utilization f, or

$$\rho = \left[\frac{\sigma_2(\gamma_1 + \gamma_2)\Sigma_f\phi_o}{(\lambda_2 + \sigma_2\phi_o)\Sigma_U}\right]\left[\frac{\Sigma_U}{\Sigma_U + \Sigma_m}\right]$$

$$= \frac{\sigma_2(\gamma_1 + \gamma_2)\Sigma_f\phi_o}{(\lambda_2 + \sigma_2\phi_o)(\Sigma_U + \Sigma_m)} = \frac{\sigma_2(\gamma_1 + \gamma_2)\Sigma_f\phi_o}{(\lambda_2 + \sigma_2\phi_o)\Sigma_R}$$

The power of the reactor during the xenon experiment was measured as 118 kw (see Appendix A). Using the latest value of the energy release per fission,[6]

$$\frac{1}{(193 \text{ Mev/fission})\ (1.60 \times 10^{-13} \text{ watts}\cdot\text{sec/Mev})}$$

$$= \frac{1}{3.088 \times 10^{-11}} \text{ fissions/sec/watt}$$

$$= 3.24 \times 10^{10} \text{ fissions/sec/watt}$$

Therefore

$$\phi_o\Sigma_f = (1.183 \times 10^5 \text{ watts})\ (3.24 \times 10^{10} \text{ fissions/sec/watt})$$

$$= 3.833 \times 10^{15} \text{ fissions/sec}$$

and

$$\rho = \frac{3.5 \times 10^{-18}\ (0.059)\ (3.833 \times 10^{15})}{\left[2.1 \times 10^{-5} + 3.5 \times 10^{-18}\ (7.36 \times 10^{11})\right]\ (8775)}$$

$$= 3.825 \times 10^{-3}$$

In order to measure the effect of xenon poisoning on the reactivity, the reactor was operated continuously at 118 kw for 72 hr and the movement of the regulating rod noted as the poison built up. Figure 10 is a plot of the change in reactivity as a function of time. The total change in reactivity as shown by the curve was 0.33% $\Delta k/k$.

The xenon run was not uneventful. The string holding the source broke early in the run, allowing the source to fall. This has been taken into account in plotting the curve. Later it was necessary to withdraw the safety rods in order to stay in the more sensitive region of the regulating rod. Readings were taken just before the safeties were moved and again immediately afterward (3 min elapsed between readings). The change in reactivity which would have been expected from the slope of the curve at this point was used to correct for the 3-min interval between the regulating rod readings.

About 24 hr before the end of the run the pool was accidently purged for about 3 hr. The effect is evident in Fig. 10 and is most serious, since the xenon concentration had obviously not reached equilibrium. There were no measurements of the pool water temperature at any time during this run and it is uncertain whether the water temperature was the same at the end of the run as when the purging was begun. Because of the negative temperature coefficient, a lower temperature would cause a lower apparent change in reactivity than actually existed and one would expect the true reactivity to be closer to that indicated by the above calculation, possibly about 0.35%.

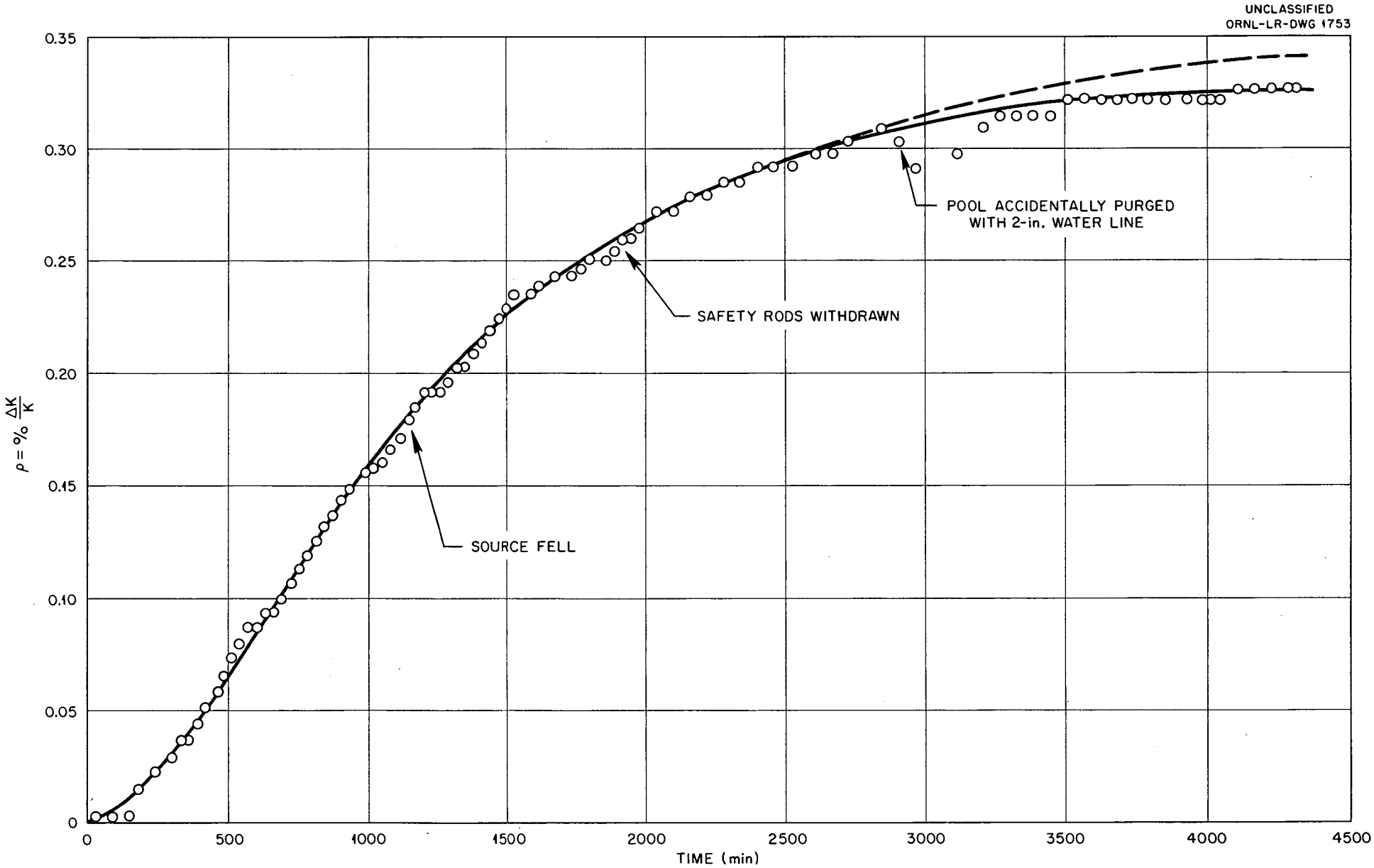

Fig. 10. Xenon Poisoning Experiment; Reactor Operation Time vs. Reactivity Change.

VII. TEMPERATURE STABILITY OF THE REACTOR

After the reactor had been operated continuously for 60 hr during the xenon run and was in complete equilibrium, the servo was shut off and the control rod left in a fixed position. The flux level held constant within 1.5% for 4 hr and apparently would have held constant much longer. Such would not be the case, of course, if the xenon poisoning were not at its equilibrium value.

Figure 11 shows a trace registered by an ionization chamber when the servo control system was off. It will be observed that in this test the power level was initially constant (far right) but, when the reactor was cooled slightly by addition of water to the pool, the power level increased. When the addition of water was stopped (far left) the power leveled off again. Thus the temperature coefficient is sufficient to make the reactor completely stable at all power levels above 10 kw. Below 10 kw the servo control system is necessary for steady operation.

In another stability experiment the reactor was brought to 100 kw and leveled off with the servo for 20 min. The rod position was noted. The power was then reduced to 100 watts and the reactor again permitted to stabilize for 20 min with the servo. The servo was then shut off and the rod was suddenly withdrawn to its former position at 100 kw. Figure 12 shows the data trace recorded by the ionization chamber. There is no

instability indicated in this test, such as overshoot or oscillation of the power level. The experiment was repeated going from 100 watts to 10 kw. Even at the lower power, the reactor quickly leveled to a stable constant power.

UNCLASSIFIED
DWG. 21169

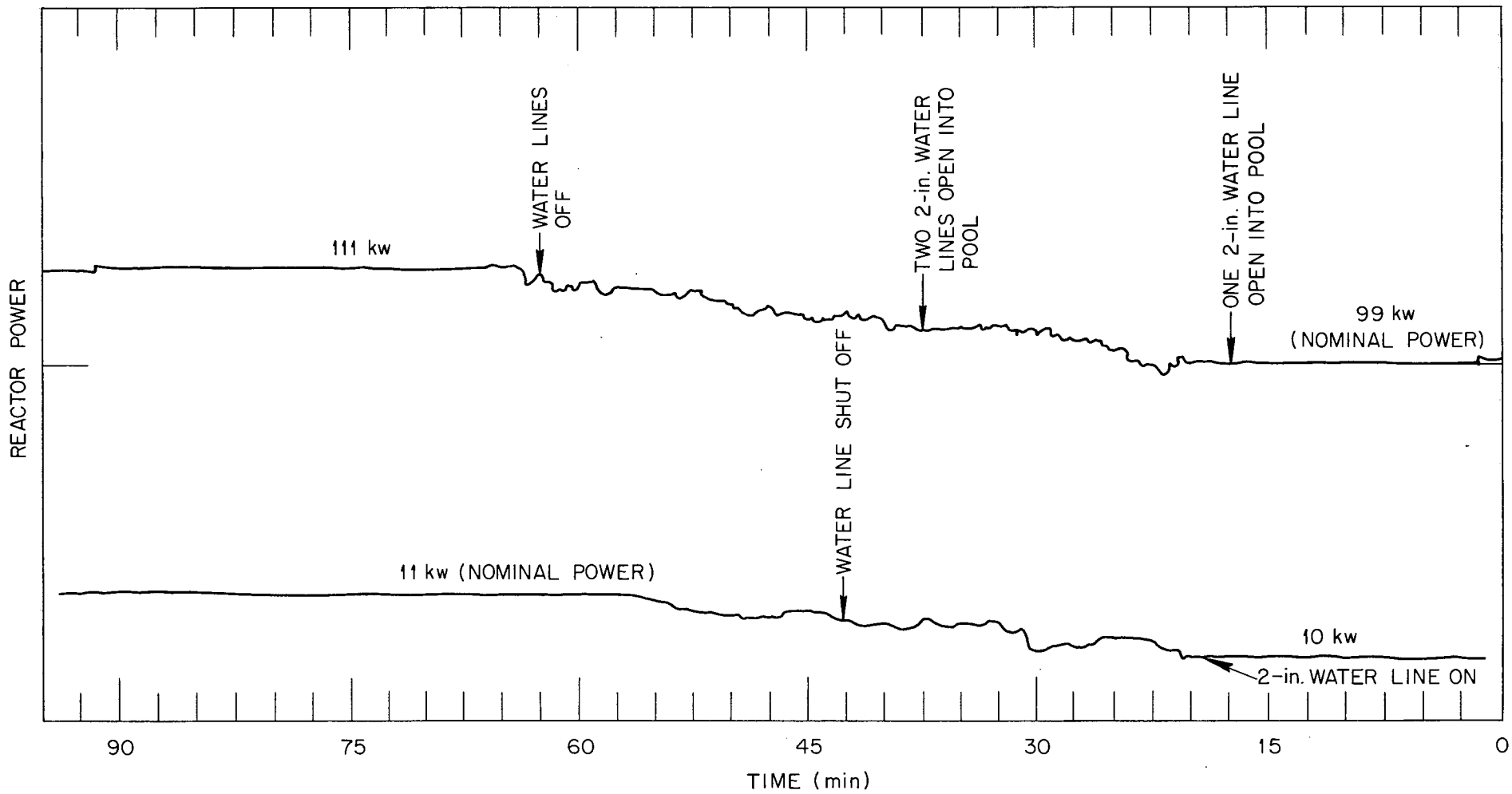

Fig. 11. Temperature Stability of the BSR; Reactor Operating Time vs. Pile Power.

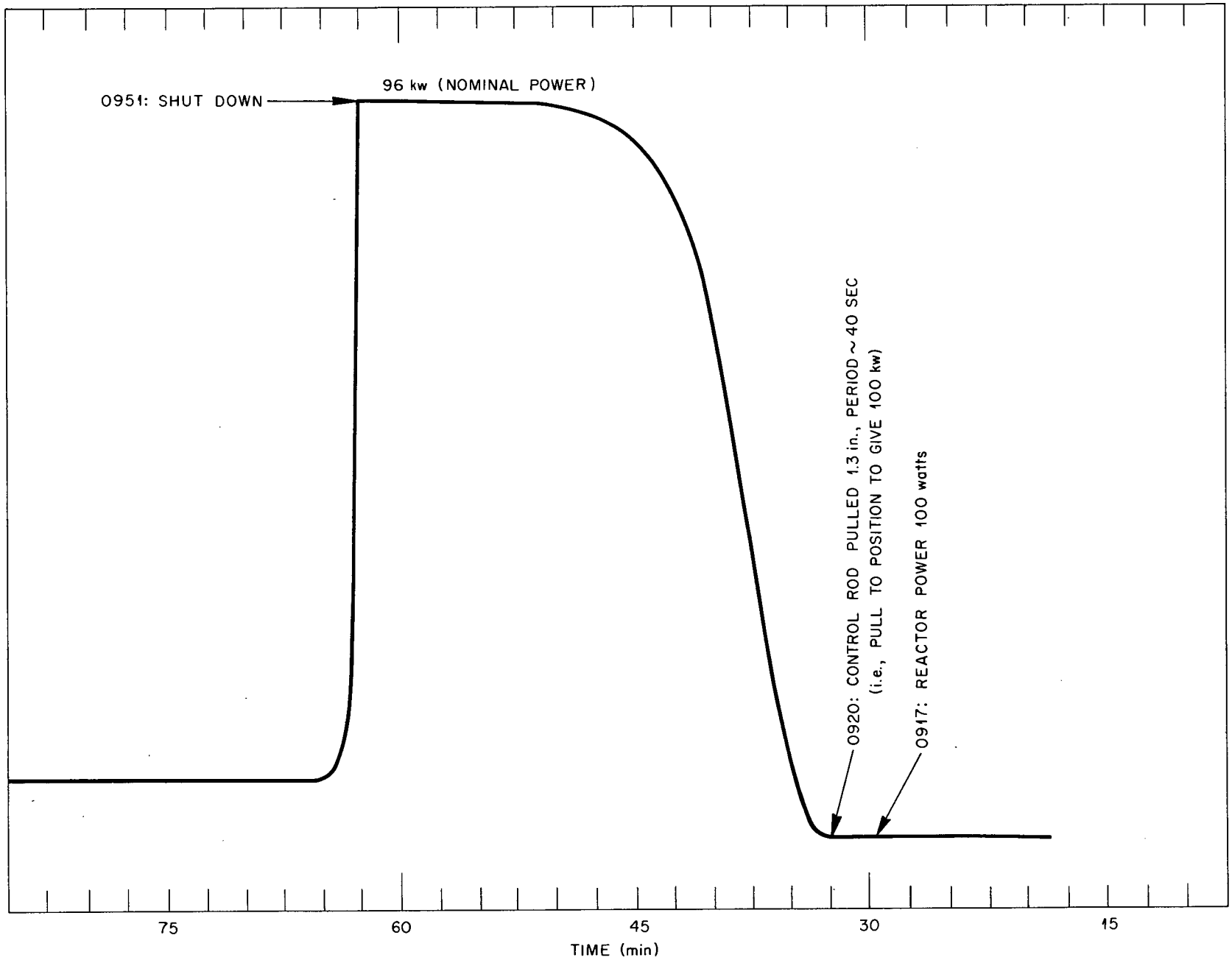

Fig. 12. Stability Test Of BSR

VIII. MEGAWATT POWER LEVEL EXPERIMENTS WITH THE BSR

There is a rather widespread interest in the Bulk Shielding or "swimming pool" type reactor with recent emphasis on higher powered versions. Typically, the University of Michigan and The Pennsylvania State University are vitally interested in higher power level information because they are contemplating building reactors of this type to operate at about 1 megawatt, which is ten times the usual maximum power level of the BSR. In addition, data on high power operation and the water activity incurred would be useful in designing the proposed "Research Reactor." Therefore, it was proposed that a controlled experiment be performed by increasing the power level of the BSR to 1 megawatt and observing the performance.

A limited amount of high power level operational data for convection cooling is available from experiments performed with the LITR.[13] However, these experiments are not entirely indicative of the performance to be expected with a "swimming pool" type reactor such as the BSR running at high power levels. The convection circulation of the LITR is very poor since, when the water circulating pump is turned off, the water that rises up through the reactor lattice by convection can only recirculate by passing down through the fuel elements. In the BSR, however, the flow can be upward in all elements because the return flow around the reactor is uninhibited. Since the

LITR, with convection cooling, reached a power level of 1.8 megawatts before boiling, it was believed that the BSR should run at a 1-megawatt power level without any difficulty.

To facilitate the observation of the reactor behavior at high power levels thermocouples were placed above and below several of the fuel elements of the reactor. These thermocouples were used to monitor the inlet and outlet water temperature (Fig.13). In addition, two gamma-ray ionization chambers were mounted directly above the reactor at the surface of the pool to monitor the radiation penetrating the water. It is known that a few milliroengtens per hour of gamma radiation penetrates the water at a power level of 100 kw but at 1000 kw the level of radiation would be much higher because of the rising activated water. Figure 14 indicates the typical radiation measurements made with a "cutie pie" portable ionization chamber around the Bulk Shielding Facility swimming pool for a power level of 100 kw. These measurements serve to show the relative radiation levels around the facility which are within Laboratory tolerance of permissible dosage. However, because of the increased convection pumping speeds, information on radiation penetrating the water at higher levels is necessary to determine the feasibility of running at these higher power levels.

The megawatt experiment was performed by increasing the BSR power level in small increments and checking at each level for any abnormal operation until a power level of 1 megawatt was achieved.

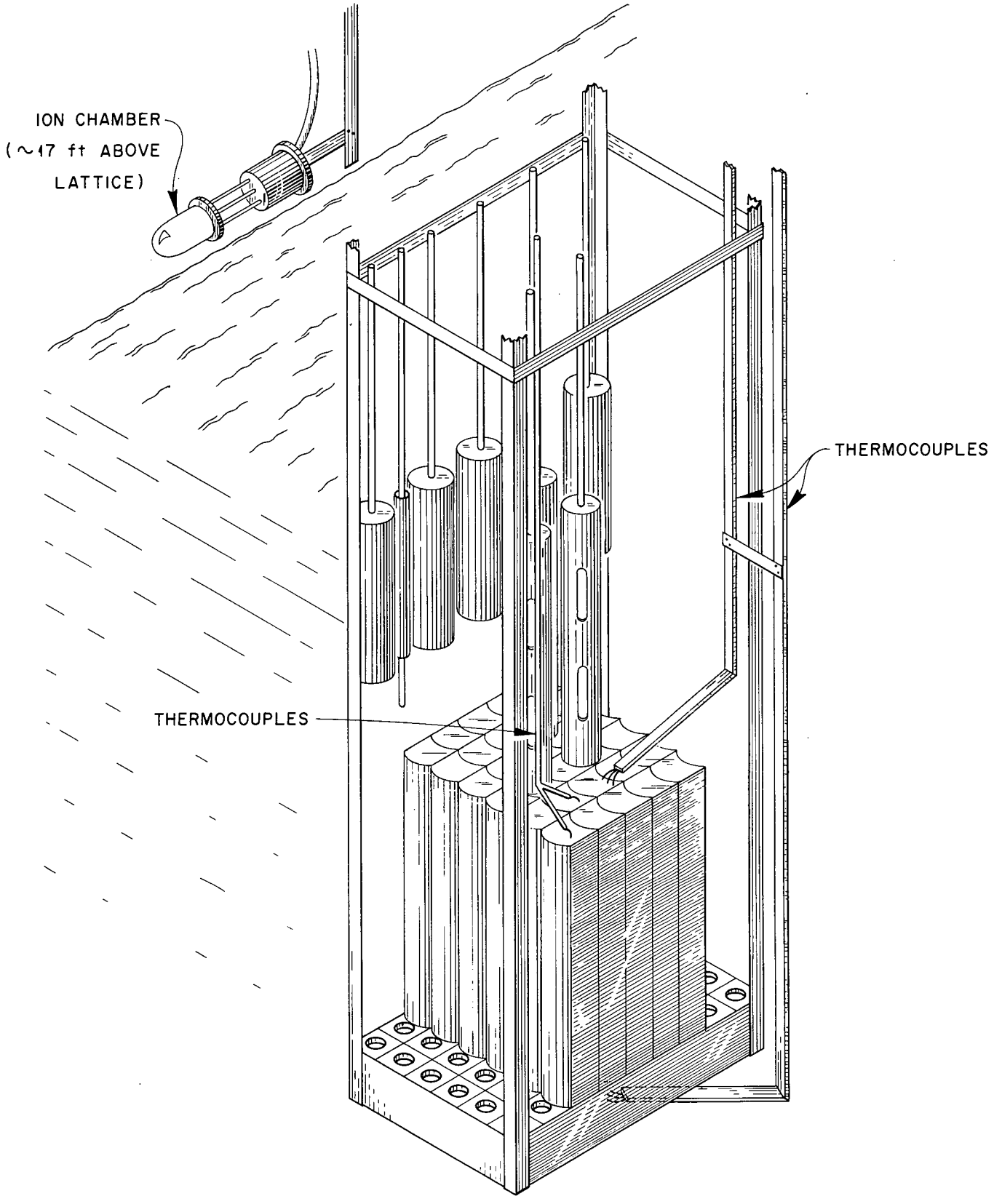

Fig. 13. BSR with Thermocouples and Ion Chamber in Position.

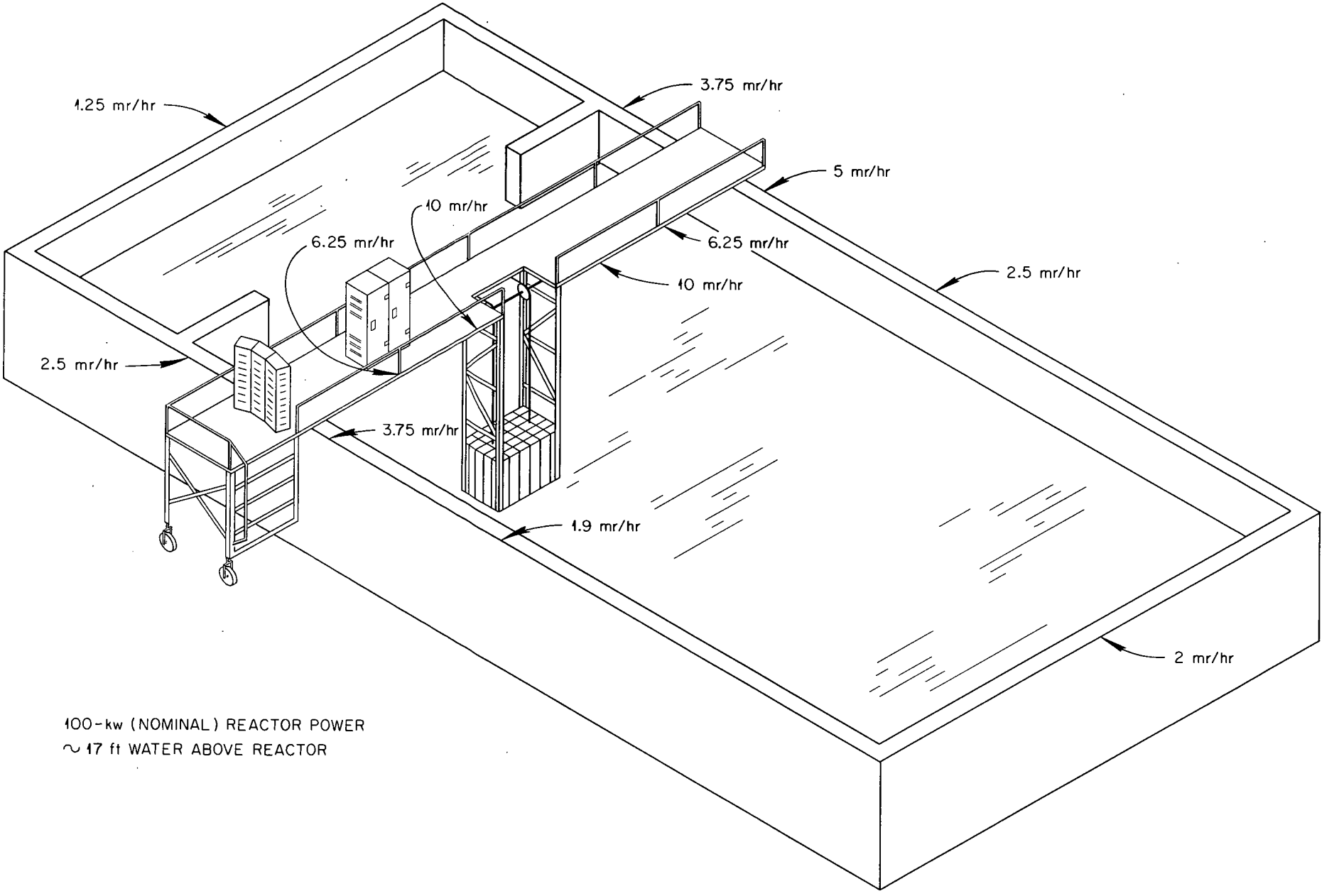

Fig. 14. Radiation Levels around Pool with BSR at 100-kw Nominal Power.

At 1 megawatt no indication of boiling could be detected, such as bubbles rising to the pool surface or an oscillation in the reactor power level. Measurements of the inlet and outlet water temperatures recorded during the experiment are given in Table 8 and plotted in Fig. 15. The difference between the inlet and the outlet water temperatures is defined as the ΔT of the reactor. For comparison purposes the ΔT measurements obtained in the Energy per Fission Experiment[6] with the BSR are also plotted in Fig. 15. These measurements are not inconsistent when it is considered that they were taken on a 19-element loading reflected with beryllium oxide in comparison to a 30-element water-reflected loading, since one would expect higher ΔT's for a given power in a smaller, more compact reactor.

As shown in Table 8, at a 1-megawatt power level the regulating rod had been withdrawn a distance corresponding to 0.45% $\Delta k/k$. This change in k is attributed mainly to the negative temperature coefficient. However, the reactor had been operated for some time ($\simeq$4 hr) at various powers above the 1-kw level at which the "0" reading was made on the regulating rod, and this operation certainly led to the buildup of a quantity of xenon whose effect would have been small but not negligible compared to the 0.45% observed $\Delta k/k$. It is interesting to note that if one applies the temperature coefficient for uniform heating of the pool water to this change in k, the effective mean temperature of the reactor at 1 megawatt is found to be about 68°C with a bulk pool temperature of 12°C. This is not now understood.

In addition to the temperature study made of the reactor during 1-megawatt operation, measurements were also made of the gamma radiation

Table 8. Thermocouple Data from 1-Megawatt Experiment

Reactor Power (kw)	Thermocouple Reading (°C)				ΔT (°C)			Regulating Rod Position (in.)	% Δk/k
	Top of Reactor			Bottom of Reactor					
	Pos. 15	Pos. 16	Pos. 7	Under Pos. 15	Pos. 15	Pos. 16	Pos. 7		
0	14	12	12	12	2	0	0		
1	14	12	12	12	2	0	0	12.85	0
10	16	16.5	12.5	12	4.0	4.5	0.5	13.3	0.035
50	19.7	17	17	12	7.7	5.0	5	14.2	0.105
100	24	23	17.5	12	12	11.0	5.5	14.95	0.170
200	27.7	27	17.5	12	15.7	15	5.5	15.8	0.240
500	41.5	41	21	12	29.5	29	9	17.5	0.375
1000	48.5	49	24	12	36.5	37	12	19.7	0.453

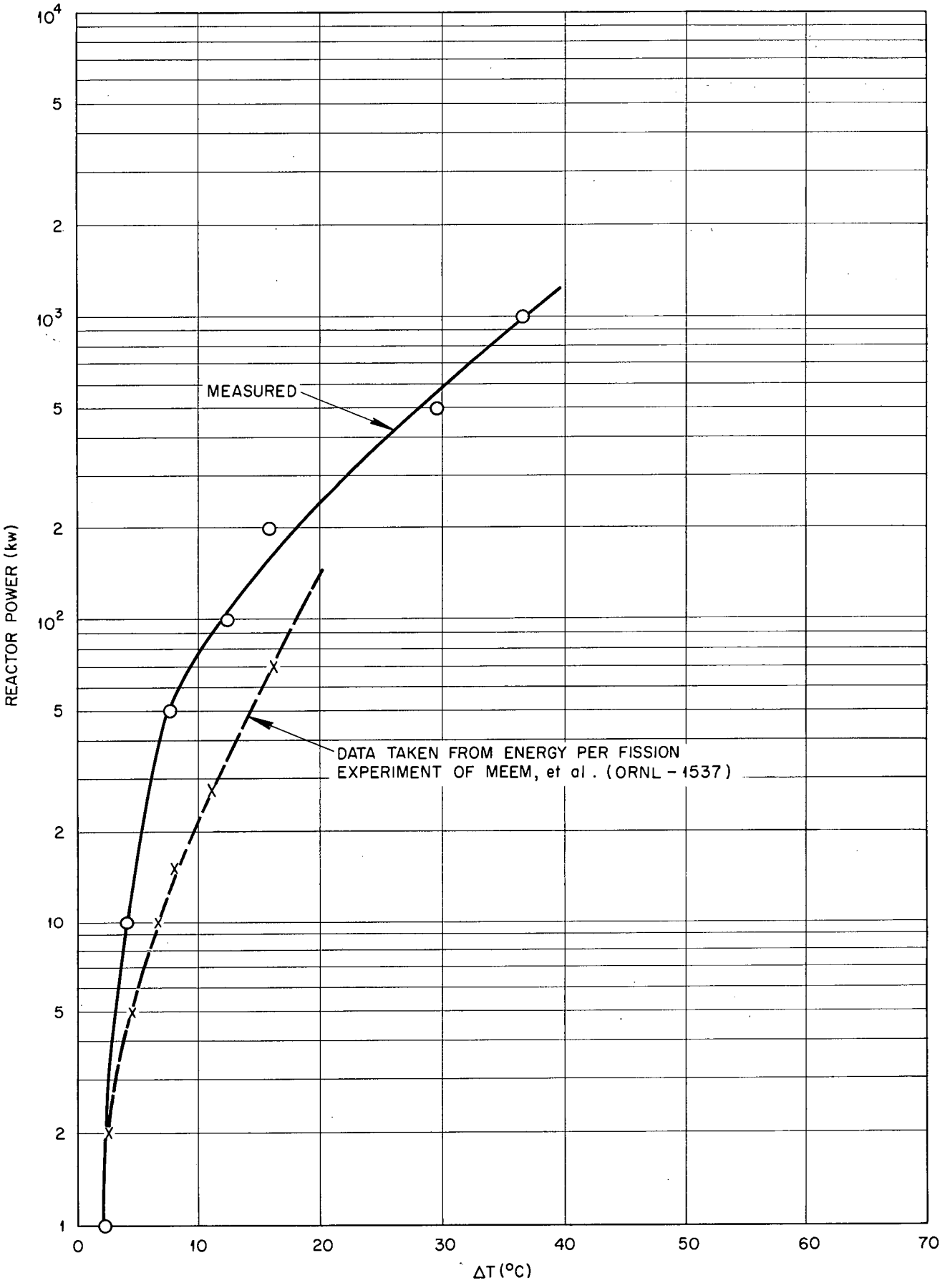

Fig. 15. Temperature Difference (ΔT) across the BSR as Measured with Thermocouples.

emerging from a position directly above the reactor at the surface of the pool. Accurate readings of the gamma-ray dose were taken with an ionization chamber at various power levels from zero to the 1-megawatt level. These measurements are reported in Table 9 and plotted in Fig. 16. In addition to the measured gamma radiation a value obtained by extrapolation of lower power experiments performed at this facility is included. This extrapolated dose would be expected to apply for the case in which essentially all the gamma radiation comes directly from the reactor. At power levels above 150 kw additional gamma radiation is contributed by the $O^{16}(n,p)N^{16} \xrightarrow{\beta} O^{16} + \gamma$ reaction. Since the water is being pumped by convection (i.e., a difference in density caused by the heating of the water as it passed up through the reactor) at a rather rapid rate through the reactor at high powers, this activated water rises rapidly to the surface, constituting the prime contributor to the gamma-ray dose at the surface of the water.

Since the gamma-ray dose at the surface was entirely too high in the above experiment a jet diffuser was designed (Fig. 17) to diffuse the water that has passed through the reactor and thus impede its rapid rise to the pool surface. The jet diffuser consisted of a framework holding six aluminum pipes 1 in. I.D. by 8 in. long pointing horizontally about 4 ft above the reactor. The 1-in. pipes were welded to a 3-in. header which was connected by a 3-in. dia fire hose to the main water line.

Gamma-ray ion chambers were placed at the water surface directly above the reactor and at several other locations around the pool, and the high-power experiment was repeated. The gamma-ray dose measurements are tabulated in Table 10 for the positions indicated in Fig. 18.

No difference in the temperature of the water passing through the reactor was noticed from the previous run.

Table 9. Gamma Radiation at the Surface of the Water Directly above the Reactor

Reactor Power (kw)	Measured Gamma-Ray Dose (mr/hr)	Calculated Gamma-Ray Dose (mr/hr) [a]
0	<1	
1	<1	
10	1	
50	3.8	
100	9.3	14
200	49	28
500	303	70
1000	1200	140

(a) Calculation based on the assumption that all gamma rays come from the reactor.

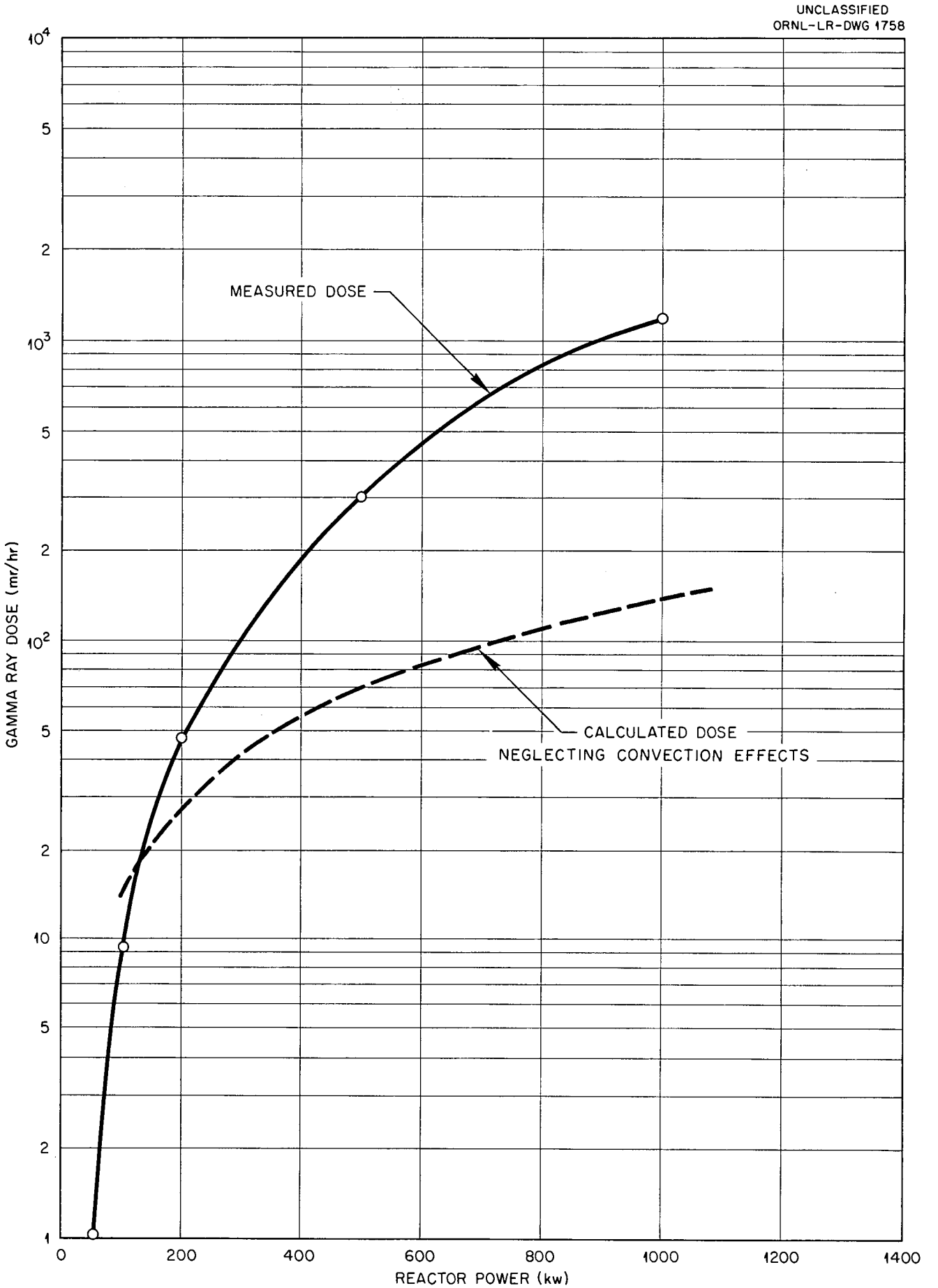

Fig. 16. Gamma Radiation at the Pool Surface Directly above the Reactor (16.5 ft above Core).

UNCLASSIFIED
ORNL-LR-DWG 2107

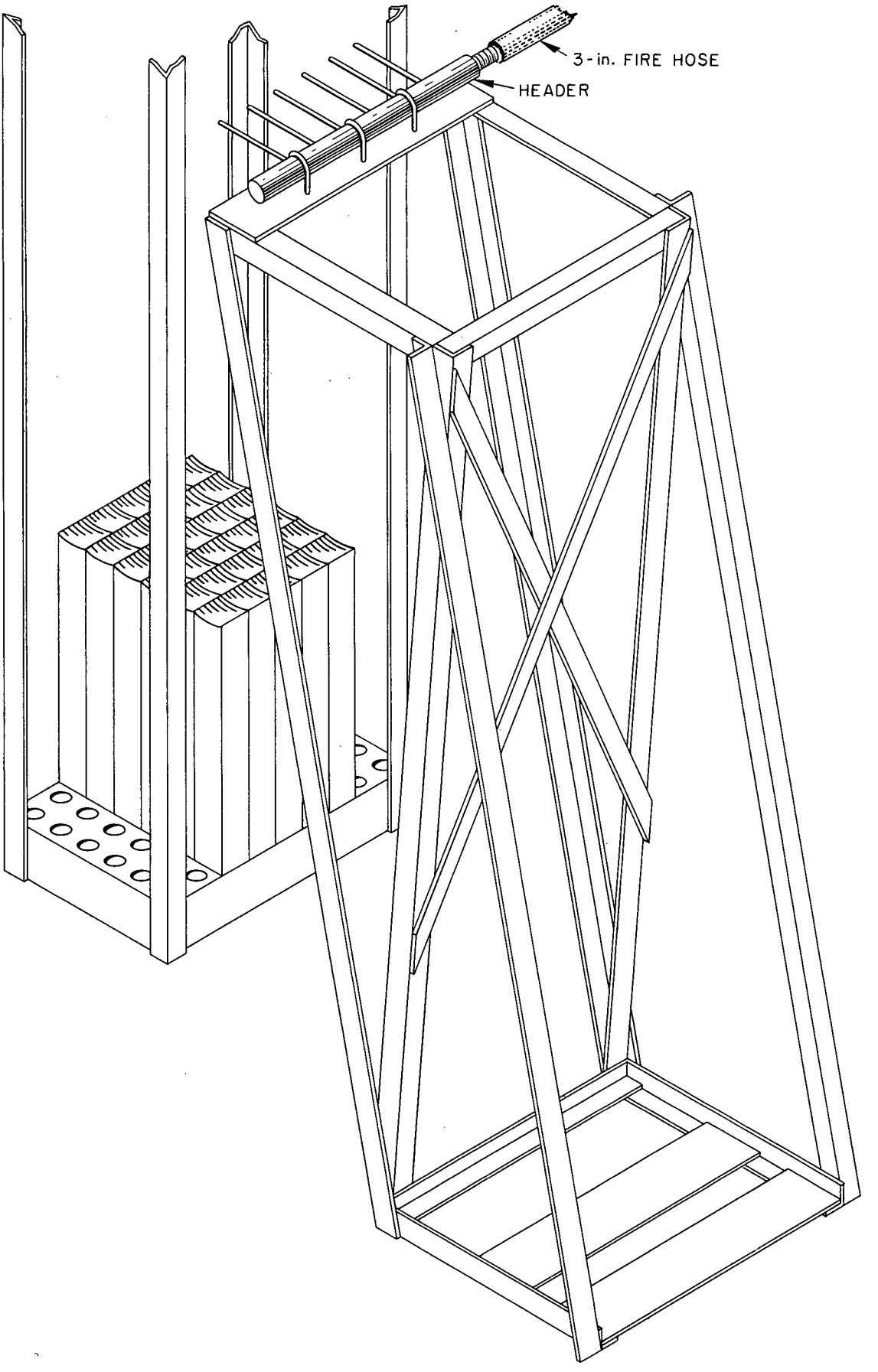

Fig. 17. Bulk Shielding Reactor with Jet Diffuser in Position.

Table 10. Gamma Radiation above the Reactor -- With and Without Jet Diffuser

Reactor Power (kw)	Gamma Radiation[a] (mr/hr)			
	Jet Diffuser On		Jet Diffuser Off	
	50-cc Ion Chamber	900-cc Ion Chamber	50-cc Ion Chamber	900-cc Ion Chamber
100	1.5			
200	10	2.5		
500	30	15		
1000	70	30	800	15

(a) 50-cc ion chamber was placed 19 1/2 in. above the water directly over the reactor; 900-cc ion chamber was placed 26 1/2 in. above the water on the south end of the pool rail.

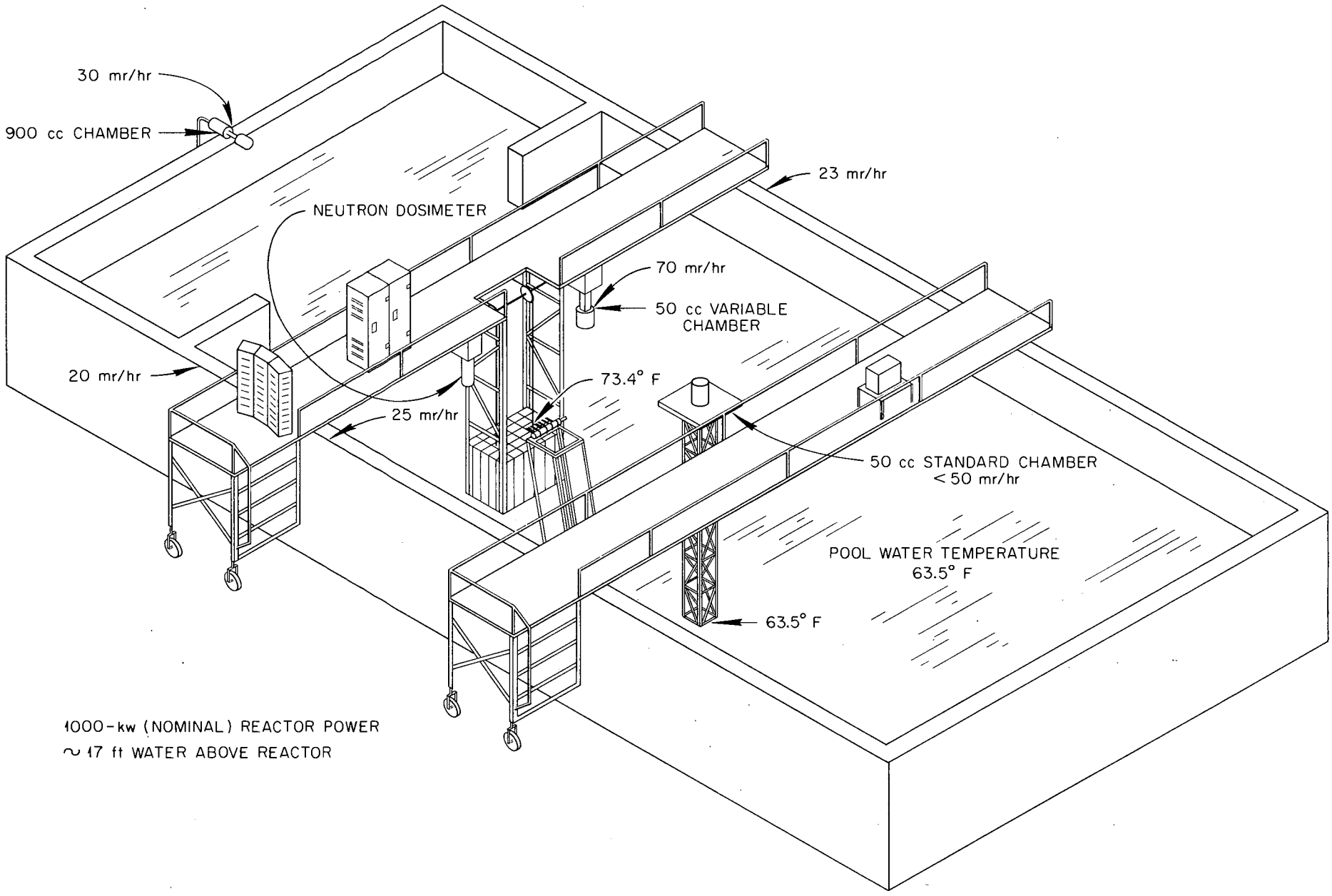

Fig. 18. Gamma Radiation from the Reactor with Jet Diffuser in Operation and Reactor at 1000 kw.

Appendix A

POWER CALCULATION FOR LOADING 22

Critical loading No. 22A was a 5 by 6 fuel element array that was symmetrical around the north-south centerline of the reactor lattice (see Fig. 1). It should be noted that two partial elements were used in this arrangement in addition to the rod elements: a half element at the center of the back (south) row of the lattice and a 110-g partial element just north of it (also on centerline) behind the regulating rod. Since this loading was completely water-reflected, the reactor could be operated at power levels ranging from 10 watts to 100 kw. The total amount of U^{235} in the lattice was 3829.23 g.

Thermal-neutron flux measurements have been completed in critical loading No. 22A (containing "hot" fuel elements) and the total power of the reactor has been calculated.

Since hot fuel elements were used in this reactor loading, it was necessary to modify the method of making flux determinations which has been reported in the past. 2S aluminum stringers were shaped to fit the space between fuel plates inside the elements, with shoulders near the top of the stringers to fix the vertical position. By means of a special handling tool these stringers were inserted into the fuel elements in place in the lattice. Foils were placed in 9/16-in. square holes cut in the stringers at centerline and at 6 and 12 in. above and below centerline. Thus a five-foil vertical traverse was measured at each exposure position within the reactor. Epicadmium activities were also measured at selected points throughout the lattice.

Cobalt foil was used as the detector material (σ = 34 barns for 2200-m/sec neutrons). Epicadmium activity measurements were necessary because of the comparatively low cadmium ratios observed (between approximately 8 and 20). Measurements were made on the east-west (curved) sides of the fuel elements by inserting the loaded stringers into the last space between the fuel plates. (The notation in the Tables A-1 and A-2 refers to the east side of the stated lattice position.)

Since both gold and cobalt have been used for making thermal-neutron flux determinations for power calibrations it was desirable to ascertain that both detector materials were indicating the same thermal flux. It was possible to run the present reactor, loaded with hot elements, at power levels ranging from 10 watts to 100 kw within an accuracy of approximately 1.5% as indicated by the BF_3 counter. Therefore it was possible for the first time at this facility to activate both gold and cobalt in precisely the same reactor positions under identical conditions except for power level. Three stringer positions within the lattice were chosen. A series of gold runs at 10 watts and of cobalt runs at 10 kw were made, resulting in four total and two epicadmium measurements with each detector material at each of six positions. The discrepancy in thermal-neutron flux as determined by each detector was less than 1%, with individual deviations ranging from 5 to 0.4%. This is well within probable experimental error. It is felt that gold and cobalt foils can be used interchangeably within the reactor lattice for thermal-neutron flux determinations.

It will be recalled[4] that the reactor power can be expressed as

$$P \text{ (watts)} = KG\ (\bar{n}v_{th})$$

Table A-1. Power Calculation for Loading 22A
10-kw nominal power
(Expt. 17)

Lattice Position	G (g of U^{235})	$\bar{\phi} \times 10^{-10}$ $\left(\frac{\text{neutrons}}{\text{cm}^2 \cdot \text{sec}}\right)$	Power per Element (watts)	Power per Row (watts)
03	138.16	5.13	302	
04	137.15	5.91	346	
05	136.10	6.47	375	
06	136.01	5.91	343	
07	139.20	5.13	304	1670
13	139.93	6.58	393	
14	138.83	7.75	459	
15	136.99	8.93	522	
16	139.11	7.75	460	
17	137.39	6.58	385	2219
23	139.60	7.80	464	
24	68.76	9.24	271	
25	138.18	10.4	613	
26	69.43	9.24	274	
27	139.61	7.80	464	2086
33	137.90	7.49	440	
34	137.21	9.07	531	
35	69.32	10.2	301	
36	137.17	9.07	530	
37	137.84	7.49	440	2242
43	138.17	6.68	394	
44	137.37	8.19	480	
45	110.19	9.34	439	
46	137.62	8.19	481	
47	137.62	6.68	392	2186
53	134.52	4.60	264	
54	138.18	5.92	349	
55	68.85	6.69	196	
56	138.17	5.92	349	
57	134.65	4.60	264	1422
		Total watts/nominal watt		11825

Table A-2. Neutron Flux Traverses through the Lattice for Loading 22A
10-kw nominal power
(Expt. 17)

East Side of Lattice Position	$\phi \times 10^{-10}$			Cadmium Ratio
	Total	Epicadmium	Thermal	
07-0	6.75	0.526	6.22	12.8
06-0	7.61	0.906	6.70	8.40
05-0	9.44	(1.12)[a]	(8.32)	(8.40)
07-6	5.54	0.423	5.12	13.1
06-6	6.07	0.733	5.34	8.28
05-6	7.17	(0.866)	(6.30)	(8.28)
07-12	3.36	0.202	3.16	16.6
06-12	4.31	0.274	4.04	15.7
05-12	5.30	(0.337)	(4.96)	(15.7)
17-0	9.20	(0.743)	(8.46)	(12.4)
16-0	9.49	1.16	8.33	8.18
15-0	12.7	1.37	11.3	9.27
17-6	7.43	(0.628)	(6.80)	(11.8)
16-6	7.47	0.925	6.54	8.08
15-6	10.0	1.09	8.91	9.17
17-12	4.57	(0.223)	(4.35)	(20.5)
16-12	5.15	0.328	4.82	15.7
15-12	7.03	0.409	6.62	17.2
27-0	10.8	(0.871)	(9.93)	(12.4)
26-0	11.9	(1.45)	(10.4)	(8.18)
25-0	15.9	1.58	14.3	10.1
27-6	8.29	(0.701)	(7.59)	(11.8)
26-6	9.36	(1.16)	(8.20)	(8.08)
25-6	12.0	1.51	10.5	7.95
27-12	5.40	(0.263)	(5.14)	(20.5)
26-12	5.72	(0.364)	(5.36)	(15.7)
25-12	7.47	1.06	6.41	7.05
37-0	9.98	0.805	9.17	12.4
36-0	11.6	(1.42)	(10.2)	(8.18)
35-0	14.7	1.67	13.0	8.80

Table A-2 Con't.

East Side of Lattice Position	$\phi \times 10^{-10}$			Cadmium Ratio
	Total	Epicadmium	Thermal	
37-6	7.94	0.671	7.27	11.8
36-6	8.92	(1.10)	(7.82)	(8.08)
35-6	11.6	1.22	10.4	9.51
37-12	4.84	0.236	4.60	20.5
36-12	6.14	(0.391)	(5.75)	(15.7)
35-12	7.66	0.532	7.13	14.4
47-0	9.22	(0.745)	(8.47)	(12.4)
46-0	10.2	(1.25)	(8.95)	(8.18)
45-0	13.3	1.31	12.00	10.2
47-6	6.97	(0.588)	(6.38)	(11.8)
46-6	7.85	(0.972)	(6.88)	(8.08)
45-6	10.4	1.01	9.39	10.3
47-12	4.26	(0.208)	(4.05)	(20.5)
46-12	5.82	(0.371)	(5.45)	(15.7)
45-12	6.85	0.273	6.58	25.1
57-0			(5.43)	
56-0			(6.66)	
55-0			(8.41)	
57-6			(4.10)	
56-6			(5.08)	
55-6			(6.66)	
57-12			(2.58)	
56-12			(3.77)	
55-12			(5.02)	

(a) Parentheses indicate calculated values, assuming a cadmium ratio.

where G is the number of grams of U^{235} in the volume over which the average thermal-neutron flux is $\overline{nv}_{th}$ and K is a constant containing the fission cross section, energy release per fission, fast fission term, and the necessary conversion factors. In previous power calibrations[4,5] K has had the numberical value of 3.944×10^{-11}. As a result of work reported in ORNL-1537,[6] this number should be 4.264×10^{-11} for flux measurements made with 1-cm^2 5-mil-thick gold foils. The new value was used in this calibration.

The activity induced in the cobalt foils was measured with the high pressure ion chamber of the Analytical Chemistry Group. The neutron flux was then calculated from the equation

$$A = N_o \phi \sigma (1 - e^{-\lambda t}) e^{-\lambda T}$$

where

A = induced activity (disintegrations/min),

N_o = number of cobalt atoms in the sample,

ϕ = neutron flux (neutrons/cm^2/sec),

σ = microscopic cross section,

λ = decay constant of the induced activity,

t = exposure time,

T = time from pile shutdown to time of measurement of activity.

If $\lambda t << 1$ and $\lambda T << 1$, this equation can be written for cobalt as

$$\phi = \frac{3.641 \times 10^6 A}{mt}$$

where

A = observed activity (disintegrations/min),

m = weight of the foil (mg),

t = exposure time (hr).

Each run was corrected for startup by the usual method,[12] and all runs were normalized together by means of the normalizing foils. Since epicadmium measurements were not made at all lattice positions, many cadmium ratios were approximated on the basis of reactor loading and previous experience.

The reactor power was computed following the method outlined by Meem and Johnson[4] with the modifications noted above. The power of reactor loading No. 22A was 11.831 kw/nominal 10 kw. Figure A-1 shows the thermal-neutron flux patterns in the lattice and Fig. A-2 shows the power distribution.

Since some of the experiments reported herein were performed with "cold" fuel elements (elements which have never been used at power levels greater than 1 watt), it was necessary to determine the difference, if any, between the hot loading and the cold loading (loading 22F). Gold foils were exposed at various positions throughout the cold reactor lattice in order to compare the flux patterns and the total power of each lattice. The cold loading, although the flux patterns were slightly different, had the same total power as the hot loading, and no additional data are included for it.

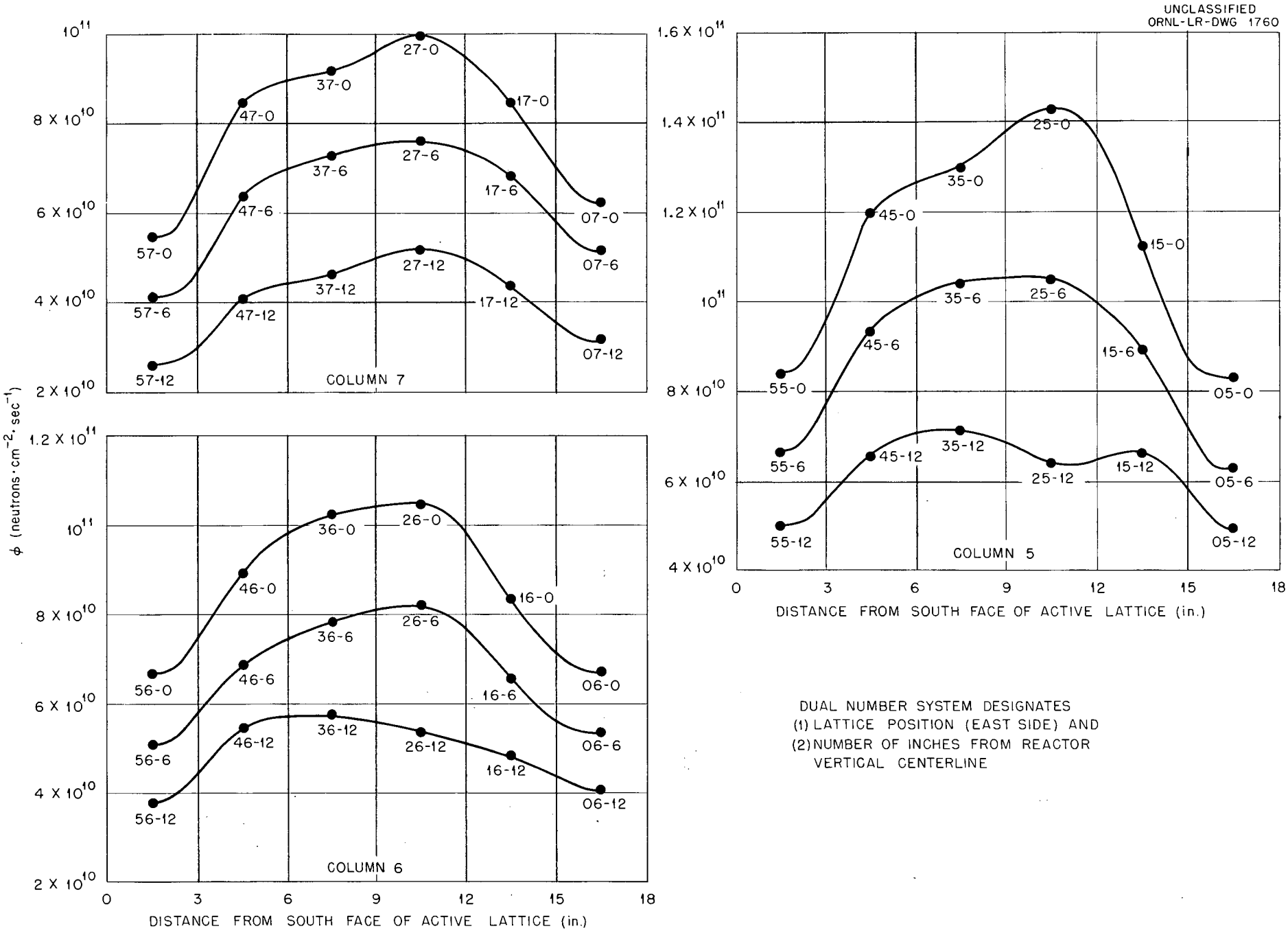

Fig. A-1. North-South Thermal-Neutron Flux Traverses by Columns in Loading 22A (10-kw Nominal Power).

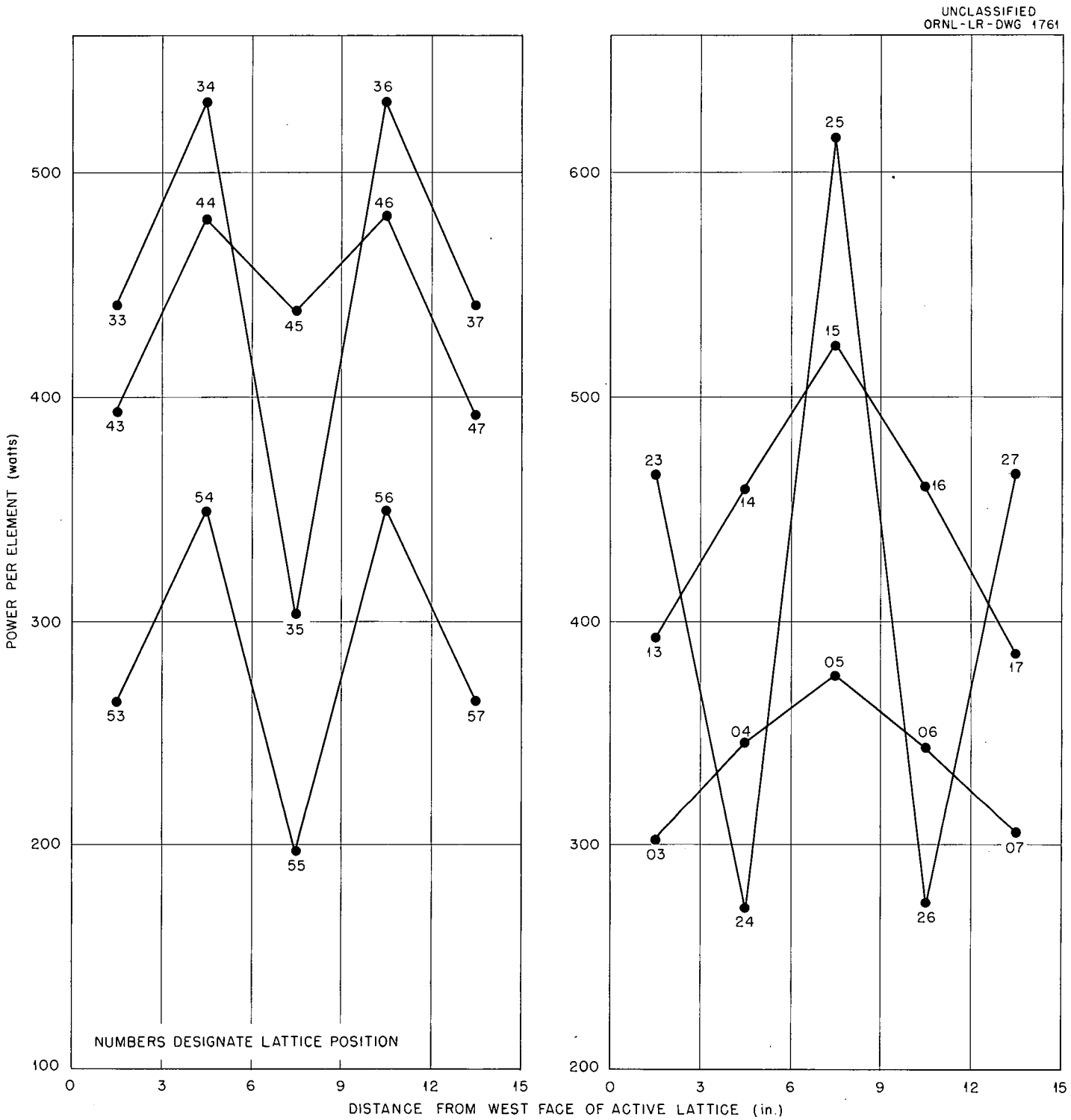

Fig. A-2. Power Distribution by Rows for Loading 22A (10-kw Nominal Power).

Appendix B

ROD CALIBRATION USING STAINLESS STEEL AS A DISTRIBUTED POISON

As described in the text, good agreement was obtained between the rod calibration using gold foils as a distributed poison and the rod calibration using the inhour formula. When using stainless steel as the poison the data was not so easy to correlate. This appendix is included to indicate the difficulties encountered.

The measurements for the calibration of the rod by poison were made with the reactor just critical ($k_{eff} = 1$), both with and without poison; therefore, the experimental observations were the amount of distributed poison equivalent to a certain rod displacement.

Using the notation of Glasstone and Edlund,[7]

$$k_{eff} = \frac{k_\infty e^{-B^2\tau}}{1 + L^2B^2} \tag{B-1}$$

Since the introduction of the stainless steel strips into the reactor displaced a not negligible amount of water from the core, it appeared that the change in Fermi age due to the presence of the steel and the corresponding absence of an equal volume of water could not be neglected.

The change in reactivity may be expressed as

$$\rho = \frac{k'_{eff} - k_{eff}}{k'_{eff}} = \frac{f'e^{-B^2\tau'} - fe^{-B^2\tau}}{f'e^{-B^2\tau'}} \tag{B-2}$$

where f is the thermal utilization. For this approximation it is assumed

that the change in the thermal leakage term, $1/(1 + L^2B^2)$, is small. From the data listed below, it is evident that this assumption is valid.

If Σ_U is the absorption cross section for uranium and Σ_R is the total absorption cross section for the reactor, then

$$f = \frac{\Sigma_U}{\Sigma_R}$$

and

$$\rho = \frac{\Delta k_{eff}}{k_{eff}} = \frac{\frac{\Sigma_U}{\Sigma'_R} e^{-B^2\tau'} - \frac{\Sigma_U}{\Sigma_R} e^{-B^2\tau}}{\frac{\Sigma_U}{\Sigma'_R} e^{-B^2\tau'}}$$

which may be reduced to

$$\rho = \frac{\Delta k_{eff}}{k_{eff}} = 1 - \left(\frac{\Sigma'_R}{\Sigma_R}\right) \left(\frac{e^{-B^2\tau}}{e^{-B^2\tau'}}\right) \qquad \text{(B-3)}$$

If the poison introduced has negligible effect on the Fermi age (as was the case with the gold foils) then Eq. (B-3) quickly reduces to

$$\rho = \frac{\Delta k_\infty}{k_\infty} = \frac{\Delta \Sigma_R}{\Sigma_R} \qquad \text{(B-4)}$$

The cross section for type 347 stainless steel used in this calibration was determined experimentally by H. Pomerance on the pile oscillator as 3.15 mm^2/g.

The following is a summary of data necessary for the calculation of the effect of distributed poison on the reactivity (see Table B-1):

Table B-1. Calculation of Total Reactor Cross Section for Loading 22A

	Volume of Components[a]			Total Volume for Active Lattice	σ_a	Total Mass of Each Component	Σ Reactor
	Full Element (cm^3)	Half Element (cm^3)	110-g Partial (cm^3)	(cm^3)	(barns)	(g)	(cm^2)
Al				45186	0.22[b]	12.200×10^4	596[c]
Core	1232	616	1234				
Side	356	356	356				
Total	1588	972	1590				
H_2O				69440	0.641[b]	69440	1489[c]
Inside	2081	2701	2081				
Outside	151	151	151				
Total	2232	2852	2232				
U	7.7	3.85	6.14	214	682[b]	3829.23	6690[c]
Total	3828	3828	3828	114840			8775[c]

(a) J. L. Meem and H. E. Hungerford, "The Unit Shield Experiments at the Bulk Shielding Facility," ORNL-1147 (Apr. 30, 1952).

(b) Cross sections for 2200-m/sec neutrons.

(c) $\Sigma_R = \frac{\rho N_o \sigma V}{A}$

Volumes occupied by constituents of the core:

Aluminum	45,186 cm^3
Water	69,440 cm^3
U^{235}	214 cm^3
Total volume of core:	1.1484×10^5 cm^3
Total weight of U^{235}:	3829 g

Total cross sections:

$$\Sigma_{Al} = 596 \text{ cm}^2; \ \sigma_a = 0.22 \text{ barns}$$

$$\Sigma_{H_2O} = 1489 \text{ cm}^2; \ \sigma_a = 0.64 \text{ barns}$$

$$\Sigma_U = 6690 \text{ cm}^2; \ \sigma_a = 682 \text{ barns}, \ \sigma_f = 575 \text{ barns}$$

$$\Sigma_R = \Sigma_U + \Sigma_{Al} + \Sigma_{H_2O} = 8775 \text{ cm}^2$$

For convenience, the experiments involving the three sets of type 347 stainless steel strips will be referred to as Cases I, II, and III. It was first necessary to calculate k_∞ and k_{eff} for the unpoisoned reactor and incidentally obtain τ, B^2, $(1 + L^2B^2)$, $e^{-B^2\tau}$, and an expression for the change in τ due to a change in the aluminum-to-water ratio. These calculations are shown in detail below:

$$k_\infty = \eta f \tag{B-5}$$

where

$$f = \frac{\text{Thermal neutrons absorbed in fuel}}{\text{Total thermal neutrons absorbed}} = \frac{\Sigma_U}{\Sigma_R}$$

and

$$\eta = \nu \frac{\Sigma_f}{\Sigma_{fuel}} \qquad (\nu = 2.5 \pm 0.1)$$

Therefore

$$k_\infty = 2.5 \left(\frac{575}{682}\right) \left(\frac{6690}{8775}\right) = 2.1078 \left(\frac{6690}{8775}\right)$$

$$= 1.6070$$

Also, by Eq. (B-1),

$$k_{eff} = \frac{k_\infty e^{-B^2\tau}}{1 + L^2B^2}$$

$$k_{eff} = \frac{1.6070\ e^{-B^2\tau}}{1 + L^2B^2}$$

where B^2 for a rectangular parallelopiped reactor is

$$B^2 = \left(\frac{\pi}{a}\right)^2 + \left(\frac{\pi}{b}\right)^2 + \left(\frac{\pi}{c}\right)^2$$

Using an extrapolation distance of 18 cm,[11]

$$a = 2.54\ (15) + 18 = 56.1 \text{ cm}$$

$$b = 2.54\ (18) + 18 = 63.72 \text{ cm}$$

$$c = 2.54\ (24) + 18 = 78.96 \text{ cm}$$

$$B^2 = 0.003136 + 0.002431 + 0.001583 = 0.00715 \text{ cm}^{-2}$$

In order to obtain τ, it is necessary to calculate the aluminum-to-water ratio for the unpoisoned reactor:

$$\frac{Al + U}{H_2O} = \frac{45186 + 214}{69440} = \frac{45400}{69440} = 0.6538$$

In ORNL-294[10] it is shown that when

$$\frac{Al}{H_2O} = 0.4, \ \tau = 46$$

and when

$$\frac{Al}{H_2O} = 0.8, \ \tau = 64$$

Therefore, assuming linearity,

$$\Delta\tau = 45\,\Delta\frac{Al}{H_2O} \qquad \text{(B-7)}$$

Thus when

$$\frac{Al + U}{H_2O} = 0.6538, \ \tau \approx 57.4$$

In ORNL-963[11] it is shown that

$$L^2 = 3.64$$

This number may be in error, but k is not very sensitive to it.

Thus,

$$1 + L^2B^2 = 1 + (3.64 \times 0.00715) = 1.02603 \approx 1.026$$

which is assumed to be a constant.

$$e^{-B^2\tau} = e^{-0.00715\,(57.4)} = e^{-0.4104} = 0.66338$$

Substituting in Eq. (B-1),

$$k_{eff} = \frac{1.6070(0.66338)}{1.026} = 1.0390$$

Obviously, for a reactor just critical, $k_{eff} = 1$. The fact that the calculated k_{eff} is 4% in error is unimportant for this discussion in that a comparison of k_{eff} with and without poison is being made, and the errors cancel. For convenience of reference, the values for the unpoisoned

reactor are collected as follows:

$$k_\infty = 1.6070$$

$$k_{eff} = 1.0390$$

$$B^2 = 0.00715$$

$$e^{-B^2\tau} = 0.66338$$

$$1 + L^2B^2 = 1.026$$

$$\Sigma_R = 8775$$

Case I.

1390.35 g of type 347 stainless steel was distributed throughout the reactor as described above. The regulating rod moved from a position of 12.1 in. with no poison to 19.1 in. with poison.

$$\text{Volume}_{ss} = \frac{1390.35}{7.8} = 178 \text{ cm}^3$$

$$\Sigma_{ss} = 1390.35 \times 0.0315 = 43.80 \text{ cm}^2$$

First, calculate the change in reactivity due to changes in thermal utilization.

$$\Sigma'_{H_2O} = 1489 \times \frac{69440 - 178}{69440} = 1489 \times \frac{69262}{69440} = 1485$$

$$\Delta\Sigma'_{H_2O} = 1489 - 1485 = 4.0$$

$$\Sigma'_R = \Sigma_R + \Sigma_{ss} - \Delta\Sigma_{H_2O}$$

$$\Sigma'_R = 8775 + 43.80 - 4$$

$$= 8815$$

$$\Delta\Sigma'_R = 8815 - 8775 = 40.00$$

Therefore

$$\frac{\Delta k_\infty}{k_\infty} = \frac{\Delta \Sigma_R}{\Sigma_R} = \frac{40.00}{8775} = 0.004558$$

Now calculate the change in reactivity due to change in Fermi age. The volume ratio of metal to water is:

$$\frac{Al + U + ss}{H_2O} = \frac{45400.0 + 178}{69262} = 0.6581$$

$$B^2 \tau' = 0.00715 \left(57.4 + 45 \Delta \frac{Al}{H_2O}\right)$$

$$= 0.00715 \left[57.4 + 45 (0.6581 - 0.6538)\right]$$

$$= 0.4118$$

$$e^{-B^2 \tau'} = 0.66246$$

$$k'_\infty = 2.1078 \times \frac{6690}{8815} = 1.5997$$

$$k'_{eff} = \frac{k'_\infty \, e^{-B^2 \tau'}}{1 + L^2 B^2}$$

$$k'_{eff} = \frac{1.5997 \, (0.66246)}{1.026} = 1.0329$$

Substituting in Eq. (B-2),

$$\frac{k'_{eff} - k_{eff}}{k'_{eff}} = \frac{1.0329 - 1.0390}{1.0329} = -0.005905$$

which should be compared with -0.0048 from the inhour calibration and should check with Eq. (B-3).

Therefore, introducing 1390.25 g of type 347 stainless steel gives a $\frac{\Delta k_{eff}}{k_{eff}} = -0.0059$ and a $\frac{\Delta k_{\infty}}{k_{\infty}} = -0.0046$. A comparison of the change in k_{eff} and the change in k_{∞} shows a difference of approximately 30%, which should represent the change in fast neutron leakage.

$$\frac{\frac{\Delta k_{eff}}{k_{eff}}}{\frac{\Delta k_{\infty}}{k_{\infty}}} = \frac{0.005905}{0.004558} = 1.295$$

The value obtained from the inhour calibration shows that the fast-neutron leakage does not change by such a large amount. It is apparent from the stainless steel experimental data and attempted calculations that this material is not too desirable for distributed poison calibrations. It will be recalled that in the calculation of the age, the assumption was made that the scattering cross sections of aluminum and stainless steel were the same and therefore that the addition of steel to the lattice would produce the same effect as the addition of an equal volume of aluminum. Although this is not a valid assumption, no effort has been made in this rough calculation to correct for the difference. Since the whole calculation is sensitive to both the buckling B^2 and the age τ, small deviations in either of these quantities will be magnified in the change in reactivity.

Case II

858.9 g of type 347 stainless steel was distributed throughout the reactor core as described above. The control rod moved from 12.2 in. with no poison to 16.3 in. with poison.

$$\text{Volume}_{ss} = \frac{858.9}{7.8} = 110.1 \text{ cm}^3$$

$$\Sigma_{ss} = 858.9\ (0.0315) = 27.05 \text{ cm}^2$$

To calculate the change in reactivity due to changes in thermal utilization:

$$\Delta\Sigma''_{H_2O} = 1489 \times \frac{110.1}{69440} = 2.360$$

$$\Sigma''_R = 8775 + 27.05 - 2.360 = 8799.7$$

$$\frac{\Delta\Sigma}{\Sigma} = 1 - \frac{\Sigma''_R}{\Sigma_R} = 1 - 1.002814 = -0.002814$$

Now calculate the change in k_{eff}:

$$B^2\tau'' = 0.00715\ (57.4 + 0.11790)$$

$$= 0.4112$$

$$e^{-B^2\tau''} = e^{-0.4112} = 0.66285$$

$$\frac{k''_{eff} - k_{eff}}{k''_{eff}} = 1 - \frac{\Sigma''_R e^{-B^2\tau}}{\Sigma_R e^{-B^2\tau''}}$$

$$\frac{\Delta k_{eff}}{k_{eff}} = 1 - \frac{8799.7\ (0.66338)}{8775\ (0.66285)} = 1 - 1.003620$$

$$= -0.003620$$

which should be compared with -0.00309 from the period calibration.

A comparison of the change in reactivity as calculated by Eq. (B-3) and by Eq. (B-4) shows a difference of approximately 30%.

$$\frac{\frac{\Delta k_{eff}}{k_{eff}}}{\frac{\Delta \Sigma}{\Sigma}} = \frac{0.003620}{0.002814} = 1.286$$

Case III

406.7 g of type 347 stainless steel was distributed throughout the reactor core. The control rod moved from 12.1 in. with no poison to 14.0 in. with poison.

$$\text{Volume}_{ss} = \frac{406.7}{7.8} = 52.1\ \text{cm}^3$$

$$\Sigma_{ss} = 406.7\ (0.0315) = 12.8\ \text{cm}^2$$

To calculate the change in reactivity due to the change in thermal utilization:

$$\Delta \Sigma'''_{H_2O} = 1489\ \left(\frac{52.1}{69440}\right) = 1.12\ \text{cm}^2$$

$$\Sigma'''_R = 8775 + 12.8 - 1.12 = 8786.7$$

$$\frac{\Sigma_R - \Sigma'''_R}{\Sigma_R} = 1 - \frac{8786.7}{8775} = 1 - 1.00133 = -0.00133$$

Now calculate the change in k_{eff}:

$$B^2\tau''' = 0.00715\ (57.4 + 0.05580)$$

$$= 0.4108$$

$$e^{-B^2\tau'''} = 0.66312$$

$$\frac{k'''_{eff} - k_{eff}}{k'''_{eff}} = 1 - \frac{8786.7\ (0.66338)}{8775\ (0.66312)}$$

$$= 1 - 1.00172 = -\ 0.00172$$

which should be compared with 0.00143 from the period calibration.

A comparison of the change in reactivity as calculated by Eq. (B-3) and by Eq. (B-4) shows a difference of approximately 30%.

$$\frac{\dfrac{\Delta k_{eff}}{k_{eff}}}{\dfrac{\Delta\Sigma}{\Sigma}} = \frac{0.00172}{0.00133} = 1.293$$

REFERENCES

(1) W. M. Breazeale, "The New Bulk Shielding Facility at Oak Ridge National Laboratory," ORNL-991 (May 8, 1951).

(2) W. M. Breazeale, "The 'Swimming Pool'-- A Low Cost Research Reactor," Nucleonics, Vol. 10, No. 11 (Nov., 1952).

(3) T. E. Cole, "Design of a Control System for a Low-Cost Research Reactor," Nucleonics, Vol. 11, No. 2 (Feb., 1953).

(4) J. L. Meem and E. B. Johnson, "Determination of the Power of the Shield Testing Reactor - I. Neutron Flux Measurements in the Water Reflected Reactor," ORNL-1027 (Aug. 13, 1951).

(5) E. B. Johnson and J. L. Meem, "Determination of the Power of the Bulk Shielding Reactor - II. Neutron Flux Measurements in Several Beryllium Oxide-Reflected Critical Assemblies," ORNL-1438 (April 21, 1953).

(6) J. L. Meem, L. B. Holland, and G. McCammon, "Determination of the Power of the Bulk Shielding Reactor - III. Measurement of the Energy Released Per Fission," ORNL-1537 (Feb. 15, 1954).

(7) Samuel Glasstone and M. C. Edlund, "The Elements of Nuclear Reactor Theory," D. Van Nostrand Company, Inc. (1952).

(8) J. A. Harvey and D. J. Hughes, "Effect of Recent Cross Section Measurements on Pile Constants," BNL-221 (Jan. 26, 1953).

(9) J. L. Meem and H. E. Hungerford, "The Unit Shield Experiments at the Bulk Shielding Facility," ORNL-1147 (April 30, 1952).

(10) L. D. Roberts and T. E. Fitch, "The Slowing Down to Indium Resonance of Fission Neutrons from a Point Fission Source in Two Mixtures of Aluminum and Light Water, 1:1 and 1:2 by Volume," ORNL-294 (Feb. 23, 1949).

(11) J. H. Buck and C. F. Leyse, "Materials Testing Reactor Project Handbook," ORNL-963 (Sept. 12, 1952).

(12) E. B. Johnson, G. McCammon, and M. P. Haydon, "Foil Measurements of Thermal Neutron Intensities in Water at the Bulk Shielding Facility," ORNL-CF-51-4-156 (April 18, 1951).

(13) W. M. Breazeale, T. E. Cole, and J. A. Cox, "Preliminary Boiling Experiment in the LITR," Reactor Sci. Technol. 2, No. 2 (Aug., 1952), TID-2002; article also published as TID-5065.